Reliability of dynamic systems in random environment by extreme value theory

M. Grigoriu and G. Samorodnitsky
Cornell University, Ithaca NY 14853–3501, USA

Abstract

A practical method is developed for estimating the performance of highly reliable dynamic systems in random environment. The method uses concepts of univariate extreme value theory and a relatively small set of simulated samples of system states. Generalized extreme value distributions are fitted to state observations and used to extrapolate Monte Carlo estimates of reliability and failure probability beyond data. There is no need to postulate functional forms of extreme value distributions since they are selected by the estimation procedure. Our approach can be viewed as an alternative implementation of the method in [7, 8] for estimating system reliability. Numerical examples involving Gaussian and non-Gaussian system states are used to illustrate the implementation of the proposed method and assess its accuracy.

1 Introduction

The probability $p_s(\tau) = P\big(X(t) \in D, 0 \le t \le \tau\big)$ that a system state $X(t)$ does not leave a safe set D during a time interval $[0, \tau]$, and the probability $p_f(\tau) = 1 - p_s(\tau)$ that $X(t)$ exits D at least once in $[0, \tau]$, referred to as reliability and failure probability, are essential quantities of interest in dynamics. They provide useful metrics for the development of economical and safe designs.

Monte Carlo simulation is the only method that can be used to find the probabilities $p_s(\tau)$ and $p_f(\tau)$ irrespective of a system size and complexity. System reliability is estimated by $\hat{p}_s(\tau) = n^{-1} \sum_{i=1}^{n} 1\big(x_i(t) \in D, 0 \le t \le \tau\big)$, where $\{x_i(t)\}$ are n independent samples of $X(t)$. However, the method is not feasible in applications involving large-dimensional ($d \gg 1$), highly-reliable ($p_f(\tau) \simeq 0$) dynamic systems because of the computational demand that can be excessive. For example, approximately 10^6 independent samples of $X(t)$ are needed to estimate failure probabilities of order 10^{-5} and the generation of these samples would require about 10^5 hours if a single sample can be obtained in 10 minutes.

To reduce the computation time for estimating $p_s(\tau)$ and $p_f(\tau)$, it has been proposed to change the measure of the state vector such that failure and survival events occur approximately in equal proportion [1]. If such measure change can be constructed, accurate estimates of $p_s(\tau)$ result from a relatively small number of samples of $X(t)$ even for highly-reliable systems. Although the Girsanov theorem provides the theoretical framework for measure change when dealing with dynamic system driven by Gaussian noise, the construction of measures providing efficient reliability estimates poses significant difficulties in applications [5] (Sect. 5.4).

Analytical solutions for $p_s(\tau)$ and $p_f(\tau)$ are available in special cases of limited practical interest. Generally, numerical methods need to be employed to calculate these probabilities. The theory of random vibration provides exact and approximate methods for calculating the reliability of dynamic systems. The exact methods involve solutions of partial differential equations, e.g., the Fokker-Plack equation and partial differential equations for the characteristic function of $X(t)$ with appropriate boundary conditions. They are practical only for dynamic systems with small state vectors [5] (Sect. 7.3). The approximate methods, e.g., the stochastic averaging, stochastic linearization, moment closure, perturbation, and crossing of random processes, have been used with mixed success to solve a broad range of applications [5] (Sect. 7.3.1.5). It is difficult to assess the accuracy of these methods in a general setting since they are based on heuristic assumptions.

Recently, an alternative method has been proposed for estimating the performance of highly-reliable dynamic systems [7, 8]. The method uses a relatively small number of independent samples of $X(t)$ to estimate the mean rate ν_D at which this process exits D, referred to as mean D-outcrossing rate, and approximate $p_s(\tau)$ from ν_D under the assumption that the D-outcrossings of $X(t)$ are Poisson events with intensity ν_D. Since the sample size is relatively small, Monte Carlo estimates of $p_s(\tau)$ based solely on samples of $X(t)$ can only be obtained for at most moderately-reliable systems. Monte Carlo estimates of mean D-outcrossing rates and concepts of the extreme value theory are employed in [7, 8] to construct approximations of $p_s(\tau)$ beyond data that can be used to assess the performance of highly-reliable systems.

This paper presents an alternative implementation of the main idea in [7, 8]. Like in these studies, our objective is to find the probabilities $p_s(\tau)$ and $p_f(\tau)$ for highly-reliable dynamic systems from a relatively small set of samples of $X(t)$. In contrast to these studies, we use exclusively the theory of univariate extreme value distribution to estimate system reliability. Our estimates of $p_s(\tau)$ and $p_f(\tau)$ are derived from generalized extreme value (GEV) and generalized Pareto (GP) distributions fitted to samples of $X(t)$. The type of the extreme value distribution used to construct our approximations for $p_s(\tau)$ and $p_f(\tau)$ does not have to be postulated. It is selected by the estimation procedure.

The proposed GEV and GP estimates of $p_s(\tau)$ and $p_f(\tau)$ are satisfactorily in all numerical examples presented in the paper. GEV estimates are more attractive since they are conceptually simple, apply to both stationary and non-stationary states, and have low storage demand. On the other hand, GP estimates involve some technicalities, apply only to stationary states in the form considered in our discussion, and may require significant storage. Our preference for GEV estimates is at variance with current estimates of floods, high wind speeds, excessive ozone levels, and other environmental extreme events that are frequently based on GP distributions [3, 10]. In this setting, GP estimates are often preferred since they have the potential of extracting more information from single records. For example, excesses of daily wind speed maxima over a specified threshold can be used to fit GP distributions and estimate wind speeds of specified return periods. Depending on the threshold, the number of these excesses can be larger or smaller than the number of years of daily wind speeds. The sample size for corresponding GEV estimates is equal to the number of years in the wind speed record.

Our results are limited to stationary state processes. Following a review of essentials of extreme value theory, the probabilities $p_s(\tau)$ and $p_f(\tau)$ are estimated for independent/dependent, Gaussian/non-Gaussian discrete-time state processes. Time series rather than stochastic processes are used to represent samples of $X(t)$ since observations of system states are recorded at discrete times.

2 Problem definition

Let $X(t)$ be an $\mathbb{R}^d$-valued stationary stochastic process defining the state of a dynamic system in the steady-state regime. Let $D_z = \{x \in \mathbb{R}^d : g(x) \leq z\}$ denote a safe set, where $g : \mathbb{R}^d \to (0, \infty)$ is a specified smooth function. The safe set D used previously to define system reliability $p_s(\tau)$ coincides with D_z for a particular value of $z > 0$. We use D_z rather then D in our further considerations since this safe set can be expanded and contracted while preserving its shape so that it can accommodate lowly- to highly-reliable systems. This definition of D_z is used to calculate the reliability of a broad range of structural/mechanical systems [2] (Chap. 6).

In this setting, our objective is to estimate the probability

$$p_s(z;\tau) = P\big(X(t) \in D_z,\ 0 \leq t \leq \tau\big) \tag{1}$$

that $X(t)$ does not leave D_z during the time interval $[0,\tau]$, referred to as system reliability. The complement $p_f(z;\tau) = 1 - p_s(z;\tau)$ of this probability is the system probability of failure.

It is assumed that (1) the system state $X(t)$ is a stationary process, (2) the information on $X(t)$ consists of samples of this process, and (3) the time interval $[0,\tau]$ is sufficiently long in a sense defined later in the paper. We develop estimates for $p_s(\tau;z)$ and $p_f(\tau;z)$ under these assumptions and construct confidence intervals on these estimates. The accuracy of the estimates depends essentially on properties of $X(t)$, available samples of these process, and the length of the reference time τ.

An alternative formulation of the reliability problem in Eq. 1 is

$$p_s(z;\tau) = P\big(Z(t) \leq z,\ 0 \leq t \leq \tau\big) = P\big(Z_\tau \leq z\big), \tag{2}$$

where

$$Z(t) = g\big(X(t)\big), \quad t \geq 0, \tag{3}$$

and $Z_\tau = \max_{0 \leq t \leq \tau}\{Z(t)\}$. The latter formulation is adequate for our objective and is used exclusively in the paper. The construction of estimates of $p_s(z;\tau)$ based on Eq. 2 is simpler since it involves concepts of the univariate extreme value theory. In contrast, estimates of this probability based on the formulation in Eq. 1 involve elements of the multivariate extreme value theory.

3 Estimates of system reliability

Generalized extreme value distributions are fitted to data and used to approximate the law of Z_τ and the probabilities $p_s(z;\tau)$ and $p_f(z;\tau) = 1 - p_s(z;\tau)$. The type of extreme value distributions used for the law of Z_τ does not have to be specified. It is selected by the estimation procedure.

Samples of system state are generated from the defining equation of $X(t)$ by Monte Carlo simulation. If the law of the stationary system state is known, stationary samples result by assuming that the initial state $X(0)$ follows the stationary distribution of $X(t)$. Otherwise, stationary samples of $X(t)$ are produced in two steps. First, samples of $X(t)$ are generated in a time interval $[0, \tau + \tau']$ starting from an arbitrary initial condition, where $\tau' > 0$ is such that transients do not extend beyond τ'. Second, sections of these samples during the time interval $[\tau', \tau + \tau']$ are kept and viewed as stationary samples of $X(t)$.

Monte Carlo estimates of $p_s(z;\tau)$ and $p_f(z;\tau)$ are not feasible when dealing with realistic, highly-reliable dynamic systems since they require large numbers of samples of $Z(t)$ and the generation of a single sample of this process is likely to be computationally demanding. Moreover, these estimates are only available in the data range. In contrast to Monte Carlo estimates, the estimates of $p_s(z;\tau)$ and $p_f(z;\tau)$ by the proposed method require relatively small numbers of samples of $Z(t)$ and extend beyond data as illustrated by the numerical examples in Sect. 4. Block maxima and threshold models are used to implement the proposed estimates of $p_s(z;\tau)$ and $p_f(z;\tau)$.

Exact, GEV and GP estimates, and asymptotic approximations of $p_f(z;m)$ are reported whenever available, e.g., exact failure probabilities are reported only for iid series. GEV and GP estimates of $p_f(z;m)$ are derived from GEV and GP distributions fitted to observations. Asymptotic approximations are theoretical distributions of extremes of $Z(t)$ corresponding to infinite reference times.

3.1 Block maxima model

Estimates of the distribution of Z_τ are constructed from independent samples $z_{\tau,i} = \max_{0\le t\le\tau}\{z_i(t)\}$, $i = 1,\ldots,n_b$, of the random variable $Z_\tau = \max_{0\le t\le\tau}\{Z(t)\}$. Resulting estimates are used to approximate system reliability and failure probability.

As previously stated, it is assumed that the exposure time τ is sufficiently long such that Z_τ can be assumed to follow a generalized extreme value distribution approximately. Otherwise, approximations of $p_s(z;\tau)$ based on the assumption that Z_τ follows a GEV distribution will be biased irrespective of the size of n_b. Since the samples of $Z(t)$ are recorded at discrete times, the available information consists of independent samples of time series $\big(Z_1 = Z(t_1),\ldots,Z_m = Z(t_m)\big)$, where $(t_1,\ldots,t_m)$ are measurement times in $[0,\tau]$. Accordingly, the probabilities $p_s(z;\tau)$ and $p_f(z;\tau)$ are referred to as $p_s(z;m)$ and $p_f(z;m)$.

3.1.1 GEV distribution

The univariate extreme value theory constructs approximations for the distribution of maxima $M_m = \max\{Y_1,\ldots,Y_m\}$ of independent identically distributed (iid) random variables $\{Y_j\}$. It can be shown that if there exist sequences of constants $\{a_m > 0\}$ and $\{b_m\}$ such that $P\big((M_m - b_m)/a_m \le y\big) \to G(y)$ as $m \to \infty$ and G is a non-degenerate distribution, then G belongs to the family of GEV distributions

$$G(y) = \exp\left\{ -\left[1 + \xi\left(\frac{y-\mu}{\sigma}\right)\right]^{-1/\xi}\right\}, \tag{4}$$

with support $\{y : 1 + \xi\,(y-\mu)/\sigma > 0\}$, where $\mu \in \mathbb{R}$, $\sigma > 0$, and $\xi \in \mathbb{R}$ are referred to as location, scale, and shape parameters [3] (Theorem 3.1.1). The subset of the GEV family with $\xi = 0$ interpreted as the limit of Eq. 4 as $\xi \to 0$ is the Gumbel family of distributions

$$G(y) = \exp\left\{ - \exp\left[- \left(\frac{y-\mu}{\sigma} \right) \right] \right\}, \quad y \in \mathbb{R}. \tag{5}$$

Note also that the supports of the GEV distributions with $\xi > 0$ and $\xi < 0$ are bounded to the left and the right, i.e., $y > \mu - \sigma/\xi$ for $\xi > 0$ and $y < \mu - \sigma/\xi$ for $\xi < 0$.

This theorem implies the approximation $P\big((M_m - b_m)/a_m \le y\big) \simeq G(y)$ provided m is sufficiently large or, equivalently,

$$P\big(M_m \le y\big) \simeq G\big((y - b_m)/a_m\big) = G^*(y), \quad \text{for large } m, \tag{6}$$

where G^* is another member of the GEV family of distributions. Generally, the GEV distributions G and G^* have different parameters. The approximation $P\big(M_m \le y\big) \simeq G^*(y)$ in Eq. 6 is particularly useful for applications since it does not involve the sequence of constants $\{a_m\}$ and $\{b_m\}$. Independent samples of M_m can be used to estimate the parameters of G^* by, for example, the maximum likelihood method. If m is not sufficiently large, the distribution of M_m may differ significantly from the GEV distributions so that the approximation in Eq. 6 is biased. Unfortunately, there are no practical methods for finding m such that $P\big(M_m \le y\big)$ can be assumed to belong to the family of GEV distributions. Useful information on the rate of convergence of $P\big(M_m \le y\big)$ to extreme value distributions can be found in [6] (Sects. 2.4 and 4.6).

Suppose $M_m = \max(Y_1, \ldots, Y_m)$ and $M_{m'} = \max(Y_1, \ldots, Y_{m'})$ follow GEV distributions. Let (μ_m, σ_m, ξ_m) and $(\mu_{m'}, \sigma_{m'}, \xi_{m'})$ denote the parameters of the GEV distributions of M_m and $M_{m'}$. If the parameters (μ_m, σ_m, ξ_m) are known, then $(\mu_{m'}, \sigma_{m'}, \xi_{m'})$ can be calculated from $\mu_{m'} = \mu_m + \sigma_m\, q^{\xi_m}/\xi_m - \sigma_m/\xi_m$, $\sigma_{m'} = \sigma_m\, q^{\xi_m}$, and $\xi_{m'} = \xi_m$, where $q = m'/m$. Hence, failure probabilities can be obtained for any time interval $[0, m']$ from the asymptotic distribution of M_m provided m' is sufficiently long such that $M_{m'}$ can be assumed to follow a GEV distribution.

The above asymptotic results for the distribution of M_m can be extended to dependent series $\{Y_j\}$ under some conditions [6] (Chap. 3). Following are examples of two sufficient conditions, referred to as D and $D(u_m)$. The condition D holds if for any integers $1 \le i_1 < \cdots < i_p < j_1 < \cdots < j_p$ for which $j_1 - i_p \ge l$ and any $u \in \mathbb{R}$ we have

$$\begin{aligned}\Delta(u) = \big| P\big(Y_{i_1} \le u, \ldots, Y_{i_p} \le u, Y_{j_1} \le u, \ldots, Y_{j_p} \le u\big) \\ - P\big(Y_{i_1} \le u, \ldots, Y_{i_p} \le u\big)\, P\big(Y_{j_1} \le u, \ldots, Y_{j_p} \le u\big) \big| \le g(l),\end{aligned} \tag{7}$$

with $g(l) \to 0$ as $l \to \infty$. The condition $D(u_m)$ requires that Eq. 7 holds for some sequences $\{u_m\}$ rather than an arbitrary u, that is, for any integers $1 \le i_1 < \cdots < i_p < j_1 < \cdots < j_p \le m$ for which $j_1 - i_p \ge l$ we have

$$\Delta(u_m) \le \alpha_{m,l}, \tag{8}$$

with $\alpha_{m,l_m} \to 0$ as $m \to \infty$ for some sequence $l_m \sim o(m)$. If there are constants $\{a_m > 0\}$ and $\{b_m\}$ such that $P\big((M_m - b_m)/a_m \le y\big)$ converges to a nondegenerate distribution

$G(y)$ and $D(u_m)$ holds for $u_m = a_m\, y + b_m$ and each y, then $G(y)$ is a GEV distribution [6] (Theorem 3.3.3). We conclude this brief review with the observation that maxima of dependent series satisfying the conditions D or $D(u_m)$ and maxima of independent series are similar in the following sense. Let $\{Y_j\}$ and $\{Y_j^*\}$ be dependent and independent stationary series that have the same marginal distribution, and set $M_m = \max(Y_1, \ldots, Y_m)$ and $M_m^* = \max(Y_1^*, \ldots, Y_m^*)$. If $\{Y_j\}$ satisfies the condition $D(u_m)$ with $u_m = a_m\, y + b_m$, then $P\big((M_m - b_m)/a_m\big) \to G(y)$ for a nondegenerate distribution G if and only if $P\big((M_m^* - b_m)/a_m\big) \to G(y)$ [6] (Theorem 3.5.2). Simpler versions of these results are available for Gaussian series (Sects. 4.2 and 4.3).

Generally, large values of dependent series tend to cluster so that the distributions of their maxima may differ from those of stationary independent series with the same marginal distributions, unless they satisfy conditions of the type stated above. The extremal index is a correction factor that can be used to obtain distributions of maxima of dependent series from distributions of maxima of independent series that have the same marginal distributions. Let $\{Y_j\}$ and $\{Y_j^*\}$ be dependent and independent stationary series that have the same marginal distribution. Under some conditions, $P\big((M_m^* - b_m)/a_m \le y\big) \to G(y)$ as $m \to \infty$, where $\{a_m > 0\}$ and $\{b_m\}$ are some sequences of constants and G is a non-degenerate distribution, if and only if $P\big((M_m - b_m)/a_m \le y\big) \to G(y)^\eta$, where $\eta \in (0, 1]$ is a constant referred to as extremal index [3] (Theorem 5.2). The inverse of η provides an approximation for the average size of clusters of extremes of $\{Y_j\}$.

3.1.2 Reliability estimates

Maximum likelihood estimates (MLE) are obtained for the parameters $\theta = (\mu, \sigma, \xi)$ of GEV distributions fitted to independent samples $\{z_{\tau,i}\}$, $i = 1, \ldots, n_b$, of Z_τ. The estimates are used to construct approximations for system reliability $p_s(z; \tau)$ and failure probability $p_f(z; \tau)$ and find confidence intervals for these probabilities.

Under the assumption that Z_τ follows a GEV distribution, the log-likelihood function for the GEV parameters has the expression [3] (Sect. 3.3.2)

$$\ell(\mu, \sigma, \xi) = -\mu\, \log(\sigma) - (1 + 1/\xi) \sum_{i=1}^{n_b} \log\left[1 + \xi\, \big((z_{\tau,i} - \mu)/\sigma\big)\right] - \sum_{i=1}^{n_b} \left[1 + \xi\, \big((z_{\tau,i} - \mu)/\sigma\big)\right]^{-1/\xi},$$

provided $\xi \neq 0$ and $1 + \xi\, (z_{\tau,i} - \mu)/\sigma > 0$, $i = 1, \ldots, n_b$. If $\xi = 0$, the log-likelihood function becomes

$$\ell(\mu, \sigma) = -n_b\, \log(\sigma) - \sum_{i=1}^{n_b} (z_{\tau,i} - \mu)/\sigma - \sum_{i=1}^{n_b} \exp\big((z_{\tau,i} - \mu)/\sigma\big).$$

The vectors $\hat{\theta}$ that maximizes $\ell(\mu, \sigma, \xi)$ or $\ell(\mu, \sigma)$ give the MLE estimates $(\hat{\mu}, \hat{\sigma}, \hat{\xi})$ of the parameters of the GEV distribution or the MLE estimates $(\hat{\mu}, \hat{\sigma})$ of the Gumbel distribution. The MLE estimator $\hat{\Theta}$ is approximately Gaussian with mean θ and covariance matrix $\gamma(\theta)$ for large n_b, where $\gamma(\theta)^{-1} = \{-\partial^2 \ell(\theta)/\partial\theta_p\, \partial\theta_q\}$ [3] (Theorem 2.2). This observation can be used to construct approximate confidence intervals for the components $\hat{\Theta}_i$ of $\hat{\Theta}$, for example, the $(1 - \alpha)$ confidence interval for $\hat{\Theta}_i$ is $\hat{\theta}_i \pm \xi_{\alpha/2} \sqrt{\gamma(\theta)_{ii}}$, where $\xi_{\alpha/2}$ is the $(1 - \alpha/2)$ quantile of the standard Gaussian variable. Since θ is not known, we replace $\gamma(\theta)$ with $\gamma(\hat{\theta})$, where $\hat{\theta}$ is an estimate of θ.

Estimates of system reliability and failure probability can be obtained by using the MLE estimates in the expression of the approximate GEV distribution of Z_τ [3] (Theorem 2.3). For example, $p_f(z;\tau)$ can be approximated by

$$p_f(z;\tau) \simeq 1 - \exp\left\{ - \left[1 + \hat{\xi}\left(\frac{z-\hat{\mu}}{\hat{\sigma}}\right)\right]^{-1/\hat{\xi}} \right\} \simeq \left[1 + \hat{\xi}\left(\frac{z-\hat{\mu}}{\hat{\sigma}}\right)\right]^{-1/\hat{\xi}}, \tag{9}$$

where the latter approximation holds for $\hat{\xi} > 0$ and $z > 0$ sufficiently large.

The delta method and the asymptotic normality of $\hat{\Theta}$ for large n_b [3] (Theorem 2.4) can be used to construct confidence intervals for $p_s(z;\tau)$ and $p_f(z;\tau)$. Denote the failure probability $p_f(z;\tau)$ by $p_f(z;\tau,\theta)$ to emphasize its dependence on θ. This probability becomes a random element if θ is replaced with $\hat{\Theta} \sim N(\theta, \gamma(\theta))$. The first order Taylor expansion of the resulting function about θ has the expression

$$\hat{P}_f(z;\tau,\hat{\Theta}) = p_f(z;\tau,\theta) + \sum_{i=1}^{3} \frac{\partial p_f(z;\tau,\theta)}{\partial \theta_i}\left(\Theta_i - \theta_i\right), \tag{10}$$

so that $\hat{P}_f(z;\tau,\hat{\Theta})$ is a Gaussian variable with mean $E\big[\hat{P}_f(z;\tau,\hat{\Theta})\big] = p_f(z;\tau,\theta) = p_f(z;\tau)$ and variance $\gamma_{p_f}(\theta) = \sum_{p,q=1}^{3} \left(\partial p_f(z;\tau,\theta)/\partial\theta_p\right)\left(\partial p_f(z;\tau,\theta)/\partial\theta_q\right)\gamma_{pq}(\theta)$. Since θ is not known, we replace it with its MLE estimate $\hat{\theta}$ and use the properties of $\hat{P}_f(z;\tau,\hat{\Theta})$ with expansion point $\theta = \hat{\theta}$ to construct confidence intervals on failure

3.2 Threshold model

In contrast to the block model that uses a single reading from an entire sample $Z(t)$, $0 \le t \le \tau$, to fit GEV distributions, the threshold model uses observations of $Z(t)$ that exceed specified thresholds. Excesses of $Z(t)$ above these thresholds are used to fit generalized Pareto distributions.

Let $Y_1, \ldots, Y_m$ be iid random variables for which there are sequences of constants $\{a_m > 0\}$ and $\{b_m\}$ such that $P\big((M_m - b_m)/a_m \le y\big)$ converges to $G(y)$ in Eq. 4 as $m \to \infty$, where $M_m = \max(Y_1, \ldots, Y_m)$ and G is the GEV distribution in Eq. 4 with location, scale, and shape parameters μ, σ, and ξ. Then, for large u,

$$P\big(Y_1 \le y \mid Y_1 > u\big) \simeq H(y) = 1 - \left(1 + \frac{\xi\,(y-u)}{\tilde{\sigma}}\right)^{-1/\xi}, \quad \text{on } \{y > u : 1 + \xi\,(y-u)/\tilde{\sigma} > 0\} \tag{11}$$

where ξ is the shape parameter of the GEV distribution G and

$$\tilde{\sigma} = \sigma + \xi\,(u - \mu). \tag{12}$$

The family of distributions $H(y)$ is called generalized Pareto (GP) [3] (Theorem 4.1).

Let $y_1, \ldots, y_m$ be m independent observations of $\{Y_i\}$ and suppose a threshold u has been selected. If $\xi \neq 0$, the log-likelihood function of the generalized Pareto parameters is

$$\ell(\tilde{\sigma},\xi) = -\left(\sum_{k=1}^{m} 1(y_k > u)\right)\log(\tilde{\sigma}) - (1 + 1/\xi)\sum_{k=1}^{m} 1(y_k > u)\,\log\left(1 + \xi\,(y_k - u)/\tilde{\sigma}\right)$$

provided $1+\xi\,(y_k-u)/\tilde{\sigma}>0$ for $y_k>u$. $k=1,\ldots,m$. If $\xi=0$, then

$$\ell(\tilde{\sigma}) = -\Big(\sum_{k=1}^{m} 1(y_k>u)\Big)\,\log(\tilde{\sigma}) - (1/\tilde{\sigma})\,\sum_{k=1}^{m} 1(y_k>u)\,(y_k-u).$$

The values of $(\tilde{\sigma},\xi)$ or $\tilde{\sigma}$ that maximize the above expressions are the MLE estimates.

The selection of the threshold u for which the above result holds is not straightforward. If u is too small, the approximation in Eq. 11 does not hold so that its use results in biased estimators. If u is too large, only a few excesses are observed so that resulting estimators of Pareto parameters will have large variances. The selection of u is commonly guided by the fact that ξ does not change with u and $\tilde{\sigma}$ varies linear with u in the range of thresholds for which Eq. 11 holds. The following two-step approach can be used to select a u. First, calculate estimates $\hat{\tilde{\sigma}}$ and $\hat{\xi}$ of $\tilde{\sigma}$ and ξ for a range of values of u. Second, identify intervals in which $\hat{\tilde{\sigma}}$ and $\hat{\xi}$ are approximately linear and constant functions of u. Thresholds in these intervals are considered to be admissible. A difficulty in applications is that intervals with these properties may be difficult to identify by visual inspection. For example, suppose $\{Y_j\}$ is an iid series with Fréchet marginal distribution $F(x)=\exp\big(-x^{-1.9}\big)$, $x>0$. Estimates of the shape parameter ξ are $\hat{\xi}=0.5016$ using $n_b=100$ blocks of size $m=1000$ and $\hat{\xi}=0.5$ using a single sample of length $n=n_b\,m=100000$ for the GEV and GP distributions, respectively. The estimates of $\tilde{\sigma}$ and ξ have the desired properties for $u\in[1,6]$. On the other hand, such an interval is difficult to identify for an iid Gaussian series $\{Y_j\}$. Using the same number of samples as for the Fréchet series, $\hat{\xi}=-0.12$ for u in the interval $[3.5,4]$ that seems to be admissible. The corresponding estimate based on block maxima is $\hat{\xi}=-0.13$. The actual value of the shape parameter is $\xi=0$ [6] (Example 1.7.1).

An alternative method has been recently developed for estimating the tail parameter [9]. The main idea is based on the fact that upper order statistics of samples that fall in the tail region behave like a Poisson random measure with a power intensity. This observation is used to construct an automated algorithm for estimating the tail index that does not require visual inspection. This method has not been used in the following numerical examples since it was possible to obtain satisfactory estimates of the tail index by method currently used in applications.

4 Numerical illustrations

Let $\{Z_i\}$, $i=1,2,\ldots$, be a real-valued stationary series defining a system state. Our objective is to estimate the probability $p_s(z;m)=P\big(\max_{1\le i\le m}\{Z_i\}\le z\big)=P\big(M_m\le z\big)$ that $\{Z_i\}$ does not exceed a critical level z, referred to as system reliability for the safe set $D_z=(-\infty,z]$ or, equivalently, system failure probability $p_f(z;m)=1-p_s(z;m)$, where $M_m=\max(Z_1,\ldots,Z_m)$ and m is a reference time. Three cases are examined. For the first two cases, $\{Z_i\}$ are independent and first order Markov sequences. For the third case, $\{Z_i\}$ are displacements of linear single degree of freedom systems recorded at discrete times. Reliability estimates are obtained by block maxima and threshold models.

The GEV and GP estimates of $p_s(z;m)$ and $p_f(z;m)$ are based on n_b independent sets of samples of $\{Z_i\}$ with size m and single samples of this series with size $n=n_b\,m$, respectively. Hence, the same number of observations of $\{Z_i\}$ are used to construct both estimates of system reliability.

The following expressions, approximations, and estimates are presented for $p_f(z;m)$. If $\{Z_i\}$ is an iid series, $p_f(z;m)$ can be calculated exactly and is reported. Generally, $p_f(z;m)$ cannot be obtained exactly for other types of time series. Theoretical GEVs, i.e., asymptotic distributions of M_m, can be constructed for iid series $\{Z_i\}$ and used to approximate $p_f(z;m)$ by $p_f(z;m) \simeq G\big((z-b_m)/a_m\big)$, where G is given in Eq. 4 and $\{a_m > 0\}$ and $\{b_m\}$ are sequences of constants depending on the marginal distribution of $\{Z_i\}$. GEV and GP estimates of $p_f(z;m)$ are estimates of $P(M_m > z)$ obtained by using block maxima and threshold models. These estimates are reported in all cases. When needed, extremal indices are used to correct GP estimates of $p_f(z;m)$ obtained under the assumptions of independence between extremes of $\{Z_i\}$.

4.1 Stationary independent series

Sequences $\{Z_i\}$ with various marginal distributions are considered. First, exact and asymptotic distributions of $M_m = \max(Z_1, \ldots, Z_m)$ are compared to find values of m below which asymptotic distributions cannot be used to characterize M_m. Second, estimates of $p_s(z;m)$ and $p_f(z;m)$ are obtained by block maxima and threshold models using the same number of observations of $\{Z_i\}$.

Example 1. Exact and asymptotic probabilities $P(M_m > z)$ are calculated and compared for iid series $\{Z_i\}$ with marginal distributions $F(z) = \Phi(z)$, $F(z) = 1 - \exp(-z)$, and $F(z) = 1/2 + (1/\pi)\tan^{-1}(z)$. The exact distribution of M_m is $P(M_m \le z) = F(z)^m$. The asymptotic distribution of M_m is the GEV distribution in Eq. 6, i.e., the limit of $P\big((M_m - b_m)/a_m \le z\big)$ as $m \to \infty$, where the scaling and shifting constants $\{a_m > 0\}$ and $\{b_m\}$ depend on the marginal distribution of $\{Z_i\}$ and are

$$
\begin{aligned}
\text{Gauss}: &\ a_m = \big(2\,\ln(m)\big)^{-1/2}; \quad b_m = 1/a_m - (1/2)\,a_m\big(\ln(\ln(m)) - \ln(\pi)\big),\\
\text{Exponential}: &\ a_m = 1; \quad b_m = \ln(m), \text{ and}\\
\text{Cauchy}: &\ a_m = 1/\tan(\pi/m); \quad b_m = 0.
\end{aligned}
$$

for the Gauss, Exponential, and Cauchy series considered in this example [6] (Sect. 1.7). The asymptotic laws of M_m are the Gumbel distribution for the Gauss and Exponential series and the Fréchet distribution for the Cauchy series.

Figures 1 to 2 show exact and asymptotic probabilities $P(M_m > z)$ with solid and dash lines, i.e., the probabilities $1 - \big(F(a_m\,z + b_m)\big)^m$ and $1 - G(z)$, where $G(z) = \exp[-\exp(-z)]$ for the Gaussian and Exponential series and $G(z) = \exp(-1/z)$ for the Cauchy series. The exact distributions approach rapidly the asymptotic distributions of M_m for exponential and Cauchy sequences. The convergence of the exact distribution to its GEV attractor is much slower for Gaussian series, a numerical observation that is consistent with statements in [6] (Sect. 2.4). The practical implication of this result is that, for a given exposure time m, M_m may or may not be assumed to follow its asymptotic GEV distribution depending on the marginal distribution of $\{Z_i\}$.

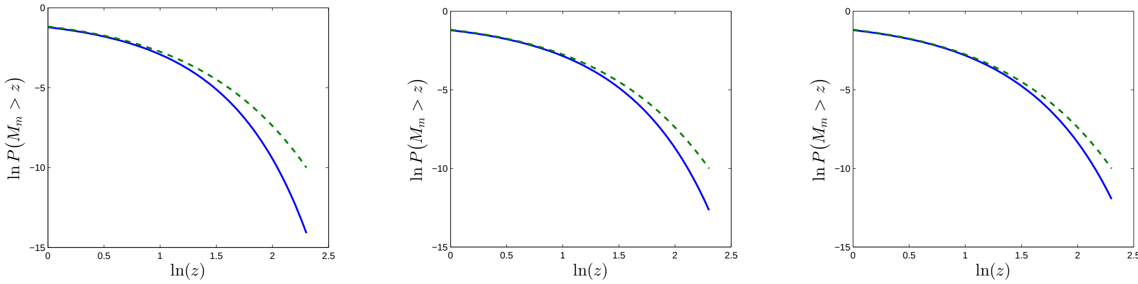

Figure 1: Exact (solid lines) and asymptotic (dash lines) probabilities $P\big(M_m > z\big)$ for standard Gaussian series with size $m = 100$ (left panel), $m = 1000$ (middle panel), and $m = 10000$ (right panel)

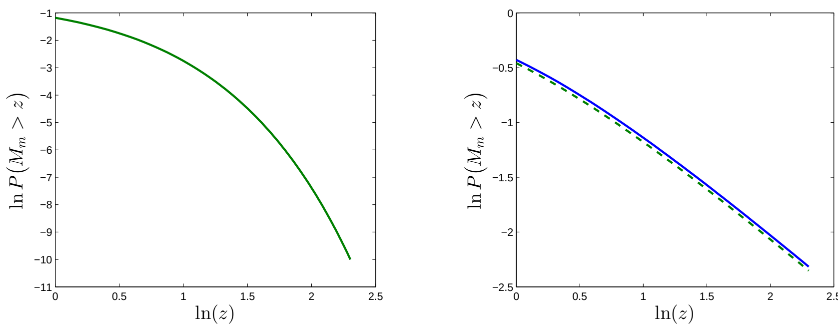

Figure 2: Exact (solid lines) and asymptotic (dash lines) probabilities $P\big(M_m > z\big)$ for exponential (left panel) and Cauchy (right panel) series with size $m = 10$. The dash and solid lines coincide in the left panel

Example 2. Suppose the iid series $\{Z_i\}$ follows a standard Gaussian distribution, an Exponential distribution with unit mean and variance, or a GEV distribution with location $\mu = 0$, scale $\sigma = 1$, and shape parameter $\xi = 0.2$. The scaling and shifting parameter for $M_m = \max(Z_1, \ldots, Z_m)$ corresponding to the GEV model are $a_m = m^{\xi}$ and $b_m = \big(a_m - 1\big)/\xi$. The scaling and shifting parameter for Gaussian and Exponential series are in the previous example. Estimates are constructed for the failure probability $p_f(z;m) = P(M_m > z)$ by using block maxima and threshold models. The data set consists of n_b sets of samples of $\{Z_i\}$ with length $m = 1000$ and single samples of this series with length $n = n_b\, m$ for the block maxima and threshold models, so that the two models use the same number of observations of $\{Z_i\}$.

Block maxima model. The dash lines in Figs. 3 to 5 have the same meaning as the dash lines in Figs. 1-2, i.e., they are asymptotic distributions of M_m. They are Gumbel for the Gaussian and Exponential series and GEV for the GEV series. The solid lines are estimates $\hat{p}_f(z;m)$ of $p_f(z;m)$ obtained by the block maxima model described in Sect. 3.1, i.e., M_m is assumed to follow a GEV distribution whose parameters are estimated from the maxima of

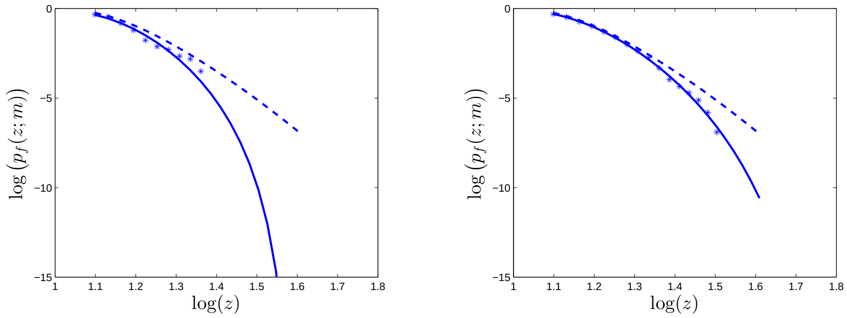

Figure 3: GEV estimates (solid lines) and asymptotic approximations (dash lines) of failure probability for Gaussian series based on $n_b = 100$ (left panel) and $n_b = 1000$ (right panel). Stars are MC estimates

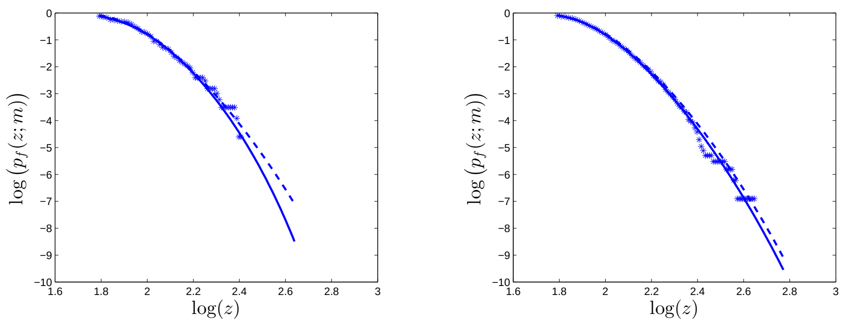

Figure 4: GEV estimates (solid lines) and asymptotic approximations (dash lines) of failure probability for Exponential series based on $n_b = 100$ (left panel) and $n_b = 1000$ (right panel). Stars are MC estimates

n_b sets of samples of $\{Z_i\}$ with length m. The GEV estimate of $p_f(z;m)$ has the expression

$$\hat{p}_f(z;m) = 1 - \exp\left\{ -\left[1 + \hat{\xi}_m \left(\frac{z - \hat{\mu}_m}{\hat{\sigma}_m}\right)\right]^{-1/\hat{\xi}_m}\right\}, \tag{13}$$

where $\hat{\mu}_m$, $\hat{\sigma}_m$, and $\hat{\xi}_m$ denote MLE estimates for the location, scale, and shape parameters of the GEV model of M_m. The MATLAB function **gevfit** was used to estimate the parameters of the above GEV distributions and corresponding confidence intervals. The stars in the figure are Monte Carlo (MC) estimates of $p_f(z;m)$ obtained from n_b samples of M_m.

The accuracy of the MLE estimates $\hat{\mu}_m$, $\hat{\sigma}_m$, and $\hat{\xi}_m$ depends on the distribution of $\{Z_i\}$, number of blocks n_b, and block length m. The MLE estimates $(\hat{\mu}_m, \hat{\sigma}_m, \hat{\xi}_m)$ are $(3.0573, 0.2773, -0.1502)$, $(3.0871, 0.2902, -0.0979)$, and $(3.0832, 0.2999, -0.0680)$ for $n_b = 100$, 1000, and 10000, respectively, if $\{Z_i\}$ is a Gaussian series. The corresponding 90% confidence intervals are

$$\begin{aligned}
&(2.9970, 3.1176), \quad (0.2385, 0.3225), \text{ and } (-0.2775, -0.0229), \quad \text{for } n_b = 100,\\
&(3.0671, 3.1071), \quad (0.2765, 0.3047), \text{ and } (-0.1389, -0.0570), \quad \text{for } n_b = 1000, \text{ and}\\
&(3.0767, 3.0897), \quad (0.2953, 0.3046), \text{ and } (-0.0804, -0.0556), \quad \text{for } n_b = 10000.
\end{aligned}$$

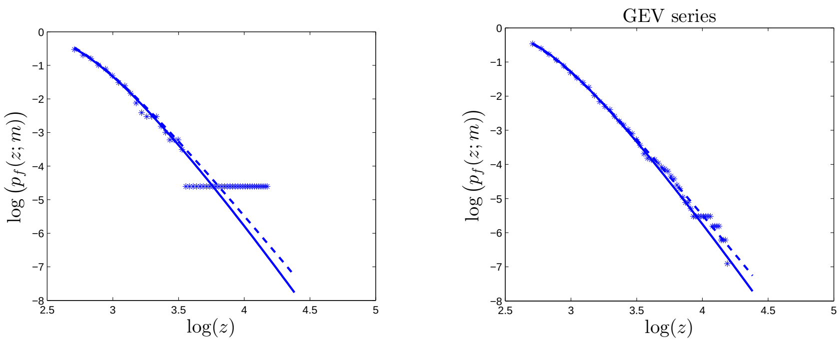

Figure 5: GEV estimates (solid lines) and asymptotic approximations (dash lines) of failure probability for GEV series based on $n_b = 100$ (left panel) and $n_b = 1000$ (right panel). Stars are MC estimates

The shape parameter of the asymptotic GEV distribution of M_m is zero since $\{Z_i\}$ is Gaussian. The estimates $\hat{\xi}_m$ are in a small vicinity of $\xi = 0$ but their confidence intervals do not contain the actual value of the shape parameter. If $\{Z_i\}$ is Exponential, $(\hat{\mu}_m, \hat{\sigma}_m, \hat{\xi}_m) = (6.8507, 1.0592, -0.0563)$ and $(6.8798, 0.9673, -0.0026)$ for $n_b = 100$ and 1000. The corresponding 90% confidence intervals are

$$(6.6161, 7.0853), \quad (0.9033, 1.2420), \text{ and } (-0.2043, 0.0917), \quad \text{for } n_b = 100 \text{ and}$$
$$(6.8125, 6.9471), \quad (0.9197, 1.0175), \text{ and } (-0.0473, 0.0421), \quad \text{for } n_b = 1000.$$

As for the Gaussian series, M_m follows approximately a Gumbel distribution for large m, i.e., a GEV distribution with shape parameter $\xi = 0$. The confidence intervals on $\hat{\xi}_m$ include the actual shape parameter in this case.

The MLE estimates for GEV series are $(\hat{\mu}_m, \hat{\sigma}_m, \hat{\xi}_m) = (14.7423, 4.0647, 0.1689)$ and $(15.0568, 4.0315, 0.1720)$ for $n_b = 100$ and 1000 for GEV series. The corresponding 90% confidence intervals are

$$(13.8447, 15.6399), \quad (3.4229, 4.8270), \text{ and } (0.0190, 0.3188)), \quad \text{for } n_b = 100 \text{ and}$$
$$(14.7761, 153375), \quad (3.8185, 4.2564), \text{ and } (0.1248, 0.2192), \quad \text{for } n_b = 1000.$$

The actual parameters of the GEV distribution of M_m are $\mu_m = (m^\xi - 1)/\xi = 14.9054$, $\sigma_m = m^\xi = 3.9811$, and $\xi_m = \xi = 0.2$. The confidence intervals contain the parameters of the GEV of M_m and are tighter for larger n_b. The horizontal lines generated by stars in the left panel of Fig. 5 is caused by a block maxima that is much larger than all the other. Similar results can be seen in other plots.

Differences between exact and asymptotic distributions of M_m are caused by the finiteness of the sample size m and the number of blocks n_b. Figures 1 and 2 show that the exact distribution of M_m approaches its GEV attractor as m increases. Since $m < \infty$, the asymptotic distribution of M_m is biased. Figures 3 to 5 illustrate effects of statistical uncertainty. The uncertainty in the estimates $(\hat{\mu}_m, \hat{\sigma}_m, \hat{\xi}_m)$ decreases with n_b. Yet, the confidence intervals on these parameters may not include the parameters of the asymptotic distribution of M_m since, if m is not sufficiently large, the asymptotic distribution is biased. An illustration is provided by the confidence intervals on $\hat{\xi}_m$ for Gaussian series.

The plots show that GEV distributions fitted to observation match Monte Carlo estimates of $P(M_m > z)$. This suggests that M_m can be assumed to follow a GEV distribution even for relatively small values of m. Figures 3 to 5 suggest that GEV distributions fitted to observation can be used to estimate failure probabilities for thresholds z way outside the data range.

Threshold model. Suppose a single samples of $\{Z_i\}$ with size $n = n_b\, m$ is available, so that we use the same number of observations for GEV and GP estimates of system reliability. The estimation procedure is outlined in Sect. 3.2.1. A range I of thresholds u is selected, MLE estimates $\hat{\xi}(u)$ and $\hat{\tilde{\sigma}}(u)$ are constructed for the parameters of the GP distribution in Eq. 11 for $u \in I$, and a threshold $u_0 \in I$ is selected such that $\hat{\xi}(u)$ is invariant and $\hat{\tilde{\sigma}}(u)$ varies linearly with u in a vicinity of u_0.

Excesses of $\{Z_i\}$ above $z > u_0$ define a Binomial sequence with probability of success $P(Z_1 > z)$. The probability $P(Z_1 > z)$ can be estimated from data for relatively low z but not for large thresholds z, as considered in our discussion. To estimate $P(Z_1 > z)$ for large thresholds z that are outside data range, observations need to be supplemented by models. Since $z > u_0$, we have $P(Z_1 > z) = P(Z_1 > u_0)\, P\big(Z_1 > z \mid Z_1 > u_0\big)$. The probability $P(Z_1 > u_0)$ can be estimated from observations since u_0 is in data range. The GP distribution for excesses of $\{Z_i\}$ above u_0 delivers the approximation

$$P\big(Z_1 > z \mid Z_1 > u_0\big) = \frac{P(Z_1 > z)}{P(Z_1 > u_0)} \simeq 1 - H(y) = \left(1 + \frac{\hat{\xi}(u_0)\, y}{\hat{\tilde{\sigma}}(u_0)}\right)^{-1/\hat{\xi}(u_0)}, \quad z > u_0, \qquad (14)$$

The probability that there is at least a success in a Binomial sequence with length m, i.e., the failure probability $p_f(z;m)$, can be approximated by

$$p_f(z;m) \simeq 1 - \exp\big[-m\, P(Z_1 > z)\big] \simeq 1 - \exp\big[-m\, P(Z_1 > u_0)\, \big(1 - H(y)\big)\big] \qquad (15)$$

provided m and $P(Z_1 > z)$ are sufficiently large and small, respectively. Under these conditions, the Binomial sequence can be approximated by a Poisson process with intensity $P(Z_1 > z)$ in the time interval $[0, m]$.

Figure 6 shows with solid lines estimates of the probability $1 - H(y)$ in Eq. 14 for

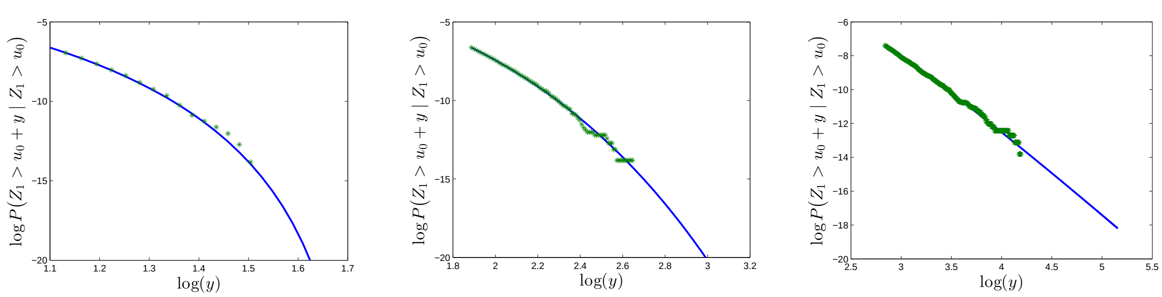

Figure 6: Estimates of $1 - H(y)$ (solid lines) for Gaussian (left panel), Exponential (middle panel), and GEV (right panel) series based on single samples of size $n = 1000000$ and corresponding MC estimates of $P\big(Z_1 > y + u_0 \mid Z_1 > u_0\big)$. Stars are MC estimates

Gaussian, Exponential, and GEV series based on single samples with length $n = n_b\, m =$

1000000 corresponding to $n_b = 1000$ sets of samples of length $m = 1000$ under the block maxima model. The thresholds u_0 are those used in the following figures, i.e., $u_0 = 2$, 6.5, and 17. The stars are MC estimates of $P\big(Z_1 > y + u_0 \mid Z_1 > u_0\big)$. The GP and MC estimates in the figure are consistent and remain consistent for other samples of $\{Z_i\}$, which suggests that the approximation in Eq. 14 is satisfactory.

The dash lines in Fig. 7 are approximations of $p_f(z;m)$ based on asymptotic distributions of M_m, i.e., $p_f(z;m) \simeq P(M_m > z) = P\big((M_m - b_m)/a_m > (z - b_m)/a_m\big)$, which is approximated by $p_f(z;m) \simeq 1 - \exp\big[-\exp\big((z - b_m)/a_m\big)\big]$ for Gaussian and Exponential series. The solid lines are GP estimates of M_m based on single samples of $\{Z_i\}$ with length $n =$

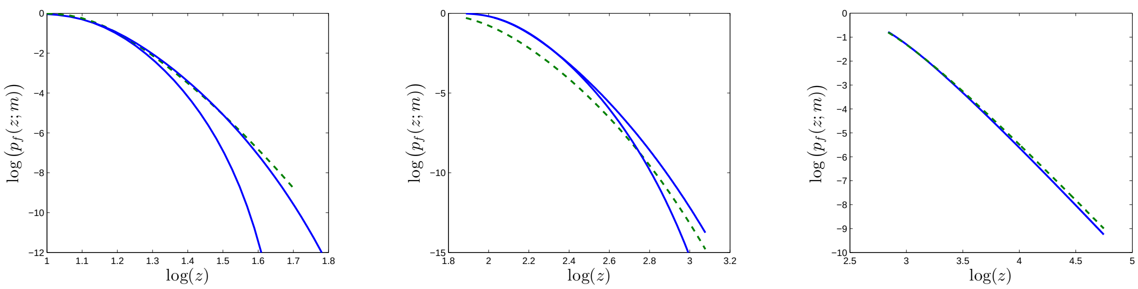

Figure 7: GP estimates (solid lines) and asymptotic approximations (dash lines) of failure probability (solid and dash lines) for Gaussian (left panel), Exponential (middle panel), and GEV (right panel) series based on single samples of size $n = 1000000$

$n_b\, m = 1000000$. The two solid lines in the left and middle panels correspond to two independent samples of $\{Z_i\}$ with size $n = 1000000$. The two lines in the right panel coincide at the figure scale. The MLE estimates for the parameters $(\xi, \tilde{\sigma})$ of the generalized Pareto (GP) distribution corresponding to one of the samples of $\{Z_i\}$ are $(-0.1132, 0.4142)$, $(0.0037, 0.9697)$, and $(0.1939, 4.2594)$ for the Gaussian, Exponential, and GEV series. The corresponding 90% confidence intervals are $(-0.1245, -0.1019)$, $(-0.0499, 0.0573)$, and $(0.0983, 0.2885)$ for the estimates of ξ and $(0.4072, 0.4214)$, $(0.9004, 1.0443)$, and $(3.7693, 4.8132)$ for the estimates of $\tilde{\sigma}$. As already mentioned, the thresholds used to obtained these estimates are $u_0 = 2$, 6.5, and 17 for the Gaussian, Exponential, and GEV series, and have been selected by the algorithm in Sect. 3.2.1. The estimates of ξ and $\tilde{\sigma}$ vary slowly with and depend linearly on u in vicinities of the thresholds u_0 selected in this manner. The MATLAB function **gpfit** was used to estimate the parameters of GP distributions and confidence intervals for these estimates.

The GEV and GP approximate distributions of M_m are consistent. For examples, the estimates of the shape parameter ξ are -0.0979 and -0.1132 for the Gaussian series, -0.0026 and 0.0037 for the Exponential series, and 0.1720 and 0.1939 for the GEV series by the block maxima and threshold models, respectively. The plots in Fig. 7 also illustrate differences in the rate of convergence of the distribution of $\max_{1 \le i \le m}\{Z_i\}$ to corresponding asymptotic distributions. The GP estimates of $P(Z_1 > z \mid Z_1 > u)$, $z > u$, in Fig. 6 match closely Monte Carlo estimates and provide models for these probabilities beyond data although $m < \infty$ so that the distribution of M_m differs from its asymptotic distribution.

We conclude this section with the following observation. The GEV and GP estimates of $p_f(z;m)$ in Example 2 and in all subsequent examples in the paper are based on the same number of observations of $\{Z_i\}$. The parameters of the GP distribution used to estimate $p_f(z;m)$ are based on excesses of $\{Z_i\}$ above a threshold u_0 that is selected by statistical arguments. Generally, the number of excesses of $\{Z_i\}$ relative to this threshold differs from n_b, i.e., the numbers of samples of $M_m = \max(Z_1, \ldots, Z_m)$ used to construct GEV estimates of $p_f(z;m)$ by the block maxima model. Suppose now that u_0 is such that the number of excesses of $\{Z_i\}$ above this threshold is approximately n_b, i.e., $u_0 \simeq \Phi^{-1}\big(1 - n_b/n\big) = 3.0902$ for $\{Z_i\}$ Gaussian, so that the GEV and GP parameters are estimated from the same number of data. The heavy solid and dash lines and the stars in Fig. 8 are those in Fig. 3. The solid thin lines are GP estimates obtained from excesses of $\{Z_i\}$ above $u_0 \simeq \Phi^{-1}\big(1 - n_b/n\big)$.

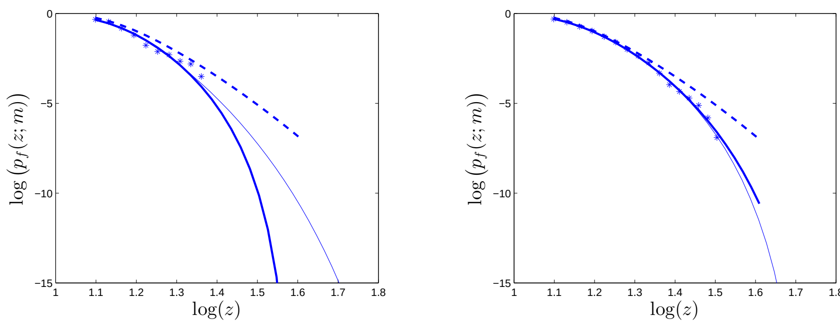

Figure 8: GEV and GP estimates (heavy and thin solid lines) and asymptotic approximations (dash lines) of failure probability for Gaussian series based on $n_b = 100$ (left panel) and $n_b = 1000$ (right panel). Stars are MC estimates

The estimates of $(\xi, \tilde{\sigma})$ are $(-0.0575, 0.2931)$ and $(-0.1138, 0.2968)$ for $n_b = 100$ and $n_b = 1000$. The 90% confidence intervals for the estimates of ξ and $\tilde{\sigma}$ are $(-0.2823, 0.1752)$ and $(0.1720, 0.3157)$ for $n_b = 100$ and $(-0.1711, -0.0566)$ and $(0.2729, 0.3228)$ for $n_b = 1000$. The GEV and GP estimates of $p_f(z;m)$ are consistent and match MC estimates of this probability. The two estimates nearly coincide as the sample size is increased from $n_b = 100$ to $n_b = 1000$ blocks. The threshold u_0 selected in this manner simplifies the implementation of GP estimates, yields accurate approximations of $p_f(z;m)$ in this illustration.

Results in this section show that, if the asymptotic law of $M_m = \max(Z_1, \ldots, Z_m)$ is the Gumbel distribution, the estimates $\hat{\xi}$ of the shape parameters of the GEV and GP estimates fitted to samples of M_m are in a small vicinity of zero. Figure 9 shows with dash and solid the Gumbel distribution with scale $\sigma = 1.3$ and location $\mu = 3$ and GEV estimates fitted to several sets of 100 (left panel) and 1000 (right panel) independent samples of this Gumbel distribution. The estimates $\hat{\xi}$ of the GEV models are in the ranges $(-0.1913, 0.0228)$ and $(-0.0384, 0.0549)$ for sets of 100 and 1000 Gumbel samples. The GEV estimates corresponding to negative values of $\hat{\xi}$ are inconsistent with the asymptotic distribution of M_m since their upper tails are bounded. Yet, they are satisfactory over a relatively large range of probabilities. The accuracy of the GEV estimates improves significantly with the sample size and the estimates show much less sample to sample variability. Two options are suggested for cases in which $\hat{\xi} \simeq 0$. If computationally feasible, increase the sample size to reduce the uncertainty in $\hat{\xi}$ and obtain reliable GEV estimates over a relatively large range of probabilities. Otherwise, use the resulting GEV estimates over a smaller range of probabilities.

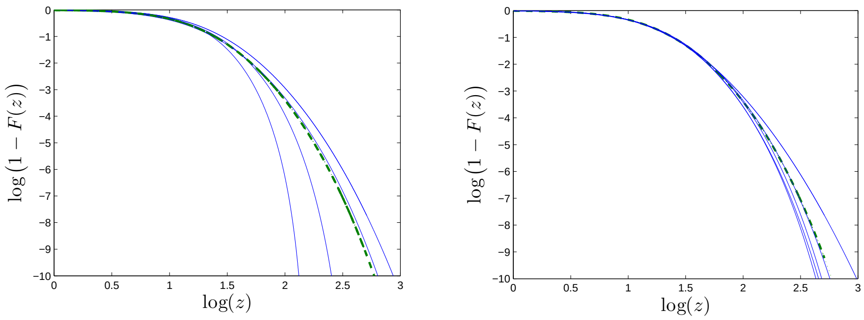

Figure 9: Gumbel distribution (dash lines) and GEV estimates (solid lines) fitted to sets of 100 (left panel) and 1000 (right panel) independent Gumbel samples

4.2 Stationary Markov series

Let $\{Z_i\}$ be the state of a dynamic system defined by the recurrence formula

$$Z_i = \rho\, Z_{i-1} + (1-\rho^2)^{1/2}\, W_i, \quad i = 1, 2, \ldots, \tag{16}$$

where $\{W_i\}$ are iid random variables with mean 0 and variance 1. The marginal distribution of $\{W_i\}$ is assumed to be Gaussian or Exponential, so that the first order Markov series $\{Z_i\}$ may or may not be Gaussian. Estimates are calculated for the failure probability $p_f(z;m)$ by the block maxima and threshold models for stationary series $\{Z_i\}$ in Eq. 16. Approximate confidence intervals are derived for estimates of $p_f(z;m)$ based on the approach in Eq. 10.

Let $\{Z_i^*\}$ be an iid series that has the same marginal distribution as $\{Z_i\}$. The asymptotic distributions of $M_m = \max_{1\le i\le m}\{Z_i\}$ and $M_m^* = \max_{1\le i\le m}\{Z_i^*\}$ may coincide under some conditions that are simple to check for Gaussian series. For example, let $r(k) = E[Z_i\, Z_{i+k}]$ denote the correlation function of a stationary Gaussian series $\{Z_i\}$. If $r(k)\log(k) \to 0$ as $k \to \infty$, then M_m follows approximately a Gumbel distribution, i.e., $P\big((M_m - b_m)/a_m \le z\big) \to \exp\big(-\exp(-z)\big)$, where $\{a_m > 0\}$ and $\{b_m\}$ are the constants for independent Gaussian series given in a previous section [6] (Theorem 4.3.3). This implies $P\big((M_m - b_m)/a_m \le z\big) \simeq P\big((M_m^* - b_m)/a_m \le z\big)$ for sufficiently large m. It can also be shown that if $r(k)\log(k) \to 0$ and $k\,\big(1-\Phi(u_k)\big)$ is bounded for a sequences of constants $\{u_k\}$, then the condition $D(u_m)$ stated in Sect. 3.1.1 holds [6] (Theorem 4.4.1).

Generally, large values of $\{Z_i\}$ cluster so that they are not independent. We have seen that, if $P\big((M_m^* - b_m)/a_m \le z\big) \to G(z)$, $m \to \infty$, where $M_m^* = \max(Z_1^*, \ldots, Z_m^*)$ and $\{Z_i^*\}$ is an iid series with the same marginal distribution as $\{Z_i\}$, then $P\big((M_m - b_m)/a_m \le z\big) \to G(z)^\eta$, where $\eta \in (0,1]$ denotes the extremal index. Since $G(z)^\eta \ge G(z)$, the failure probability $p_f(z;m) \simeq 1 - G(z)^\eta \le 1 - G(z)$ will be overestimated if clustering of large value of $\{Z_i\}$ is disregarded. Designs based on the independence assumption for $\{Z_i\}$ will be conservative. The degree of conservatism may or may not be significant depending on the properties of $\{Z_i\}$ and the reliability level.

Example 3. Suppose $\{W_i\}$ in Eq. 16 is Gaussian and the initial state is a standard Gaussian variable that is independent of the driving noise, so that $\{Z_i\}$ is a stationary Gaussian series. Since $\{Z_i\}$ is a Gaussian series with correlation function $r(k) = E[Z_i\, Z_{i+k}] = \rho^{|k|}$ and

$r(k)\log(k) \to 0$ as $k \to \infty$, we have $P\big((M_m - b_m)/a_m \le z\big) \to \exp\big(-\exp(-z)\big)$, where $\{a_m > 0\}$ and $\{b_m\}$ are the constants for independent Gaussian series given in a previous section [6] (Theorem 4.3.3). This implies that the extremal index for this series is $\eta = 1$ and the asymptotic distributions of M_m and M_m^* coincide.

Block maxima model. The approach for estimating the distribution of M_m is identical with that used for independent series since the samples of M_m, i.e., block maxima, are independent. It is assumed as previously that m is sufficiently large such that M_m follows approximately a GEV distribution. A useful discussion on the rate at which the distributions of maxima of stationary Gaussian series converge to the Gumbel distributions can be found in [6] (Sect. 4.6).

The solid and dash lines in Fig. 10 are Monte Carlo (MC) and GEV estimates of

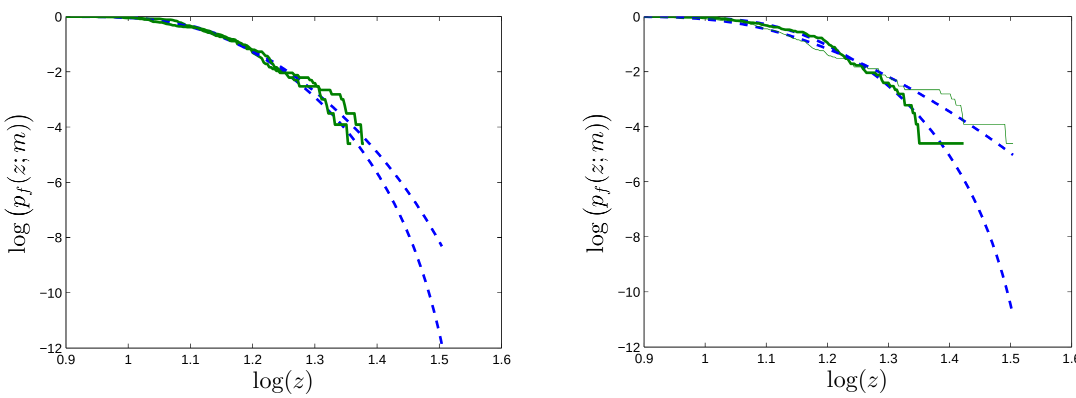

Figure 10: Estimates of $p_f(z;m)$ for $\rho = 0.0$ (left panel) and $\rho = 0.7$ (right panel) for two sets of $n_b = 100$ samples with length $m = 1000$ by MC (solid lines) and GEV (dash lines)

$p_f(z;m) = P\big(M_m > z\big)$ for $m = 1000$ obtained from two sets of $n_b = 100$ independent samples of $(Z_1, \ldots, Z_m)$. The MLE estimates $(\hat{\mu}, \hat{\sigma}, \hat{\xi})$ of the GEV parameters (μ, σ, ξ) for the two sets of $n_b = 100$ samples of $(Z_1, \ldots, Z_m)$ are

$$(3.0679, 0.2560, -0.1027) \text{ and } (3.0439, 0.2683, -0.1551), \quad \text{for } \rho = 0.0 \text{ and}$$
$$(3.1015, 0.2800, -0.1679) \text{ and } (3.0038, 0.3249, -0.0351), \quad \text{for } \rho = 0.7.$$

The estimates of $p_f(z;m)$ can differ significantly for large thresholds z, i.e., highly reliable systems, if based on $n_b = 100$ blocks. The number of blocks needs to be increased to obtain reliable estimates for failure probabilities up to, e.g., order 10^{-10}. For example, MLE estimates $(\hat{\mu}, \hat{\sigma}, \hat{\xi})$ of the GEV parameters based on $n_b = 10000$ independent samples of $(Z_1, \ldots, Z_m)$ exhibit less sample-to-sample variability. For two sets of $n_b = 10000$ blocks these estimates are $(3.0886, 0.2982, -0.0663)$ and $(3.0882, 0.2974, -0.0545)$ if $\rho = 0.0$ and $(3.0163, 0.3235, -0.0877)$ and $(3.0204, 0.3284, -0.0891)$ if $\rho = 0.7$. The corresponding estimates of $p_f(z;m)$ based on these sets of samples of $\{Z\}$ nearly coincide for failure probabilities up to order 10^{-10}. As for results in Figs. 4 and 5, the GEV estimates in Fig. 10 match closely Monte Carlo estimates of $p_f(z;m)$ and provide simple models for extending MC estimates of $p_f(z;m)$ beyond data.

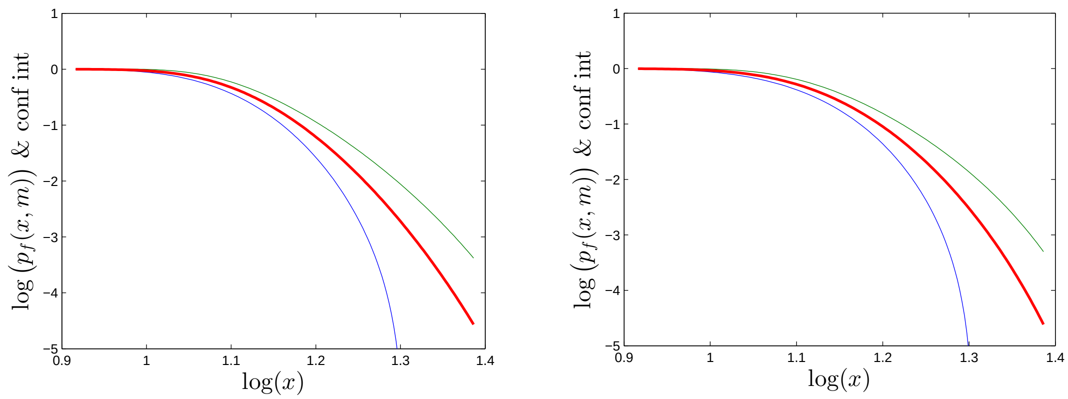

Figure 11: Approximate 90% confidence intervals for the MLE estimator of $p_f(z;m)$ for $m = 1000$, $n_b = 100$, $\rho = 0.0$ (left panel) and $\rho = 0.7$ (right panel)

Figure 11 shows symmetric 90% confidence intervals for the estimator of the failure probability in Eq. 10 based on $n_b = 100$ independent samples of $(Z_1, \ldots, Z_m)$, $m = 1000$, with correlation coefficients $\rho = 0.0$ and $\rho = 0.7$. They correspond to one of the sets of samples used in Fig. 10. The confidence intervals for $\rho = 0.7$ are slightly larger than those for $\rho = 0.0$ for this numerical illustration.

Threshold model. The procedure used to estimate $p_f(z;m)$ for stationary independent Gaussian series holds in this case since $\{Z_i\}$ is a stationary Gaussian series and its correlation function $r(k)$ satisfies the condition $r(k)\log(k) \to 0$ as $r \to \infty$. Estimates $\hat{\xi}(u)$ and $\hat{\tilde{\sigma}}(u)$ are calculated for the parameters ξ and $\tilde{\sigma}$ of the GP distributions corresponding to excesses of $\{Z_i\}$ above thresholds u in an interval I, a threshold $u_0 \in I$ is selected following the approach in Example 2, the conditional probability $P(Z_1 > z \mid Z_1 > u_0)$, $z > u_0$, is approximated by Eq. 14, and an estimate of $p_f(z;m)$ results from Eq. 15.

MLE estimates $(\hat{\xi}, \hat{\tilde{\sigma}})$ of the GP parameters are $(-0.1347, 0.4160)$ and $(-0.1430, 0.4225)$ for $\rho = 0.0$ and $\rho = 0.7$, respectively, and a sample of $\{Z_i\}$ with length $n = 100000$. The corresponding 90% confidence intervals on $\hat{\xi}$ and $\hat{\tilde{\sigma}}$ are $(-0.1707, -0.0988)$ and $(0.3940, 0.4392)$ for $\rho = 0$ and $\hat{\tilde{\sigma}}$ are $(-0.1760, -0.1100)$ and $(0.4011, 0.4451)$ for $\rho = 0.7$. The estimates are for a threshold $u_0 = 2$. The quality of these estimates improves significantly if based on a sample of length $n = 1000000$. For $\rho = 0.0$ the MLE estimates of $(\xi, \tilde{\sigma})$ are $(-0.0987, 0.3616)$ and 90% confidence intervals on $\hat{\xi}$ and $\hat{\tilde{\sigma}}$ are $(-0.1188, -0.0786)$ and $(0.3511, 0.3725)$, respectively. They suggest that $\hat{\xi}$ approaches zero as n increases, which is the shape parameter for the Gumbel distribution.

Monte Carlo (MC), GEV, and GP estimates of $p_f(z;m)$ are shown in Fig. 12 with solid lines, dash lines, and circular markers. The solid and dash lines are those from Fig. 10. The MC and GEV estimates are obtained from sets of $n_b = 100$ samples of $\{Z_i\}$ with length $m = 1000$ while the GP estimates are derived from single samples of $\{Z_i\}$ with length $n = n_b\, m = 100000$. The GEV and GP estimates show larger sample-to-sample variability for correlated series. Also, differences between GEV and GP estimates seem to increase with the correlation of $\{Z_i\}$. The GEV and GP estimates have a common feature, which is essential for estimating performance of highly-reliable systems. In contrast to MC estimates

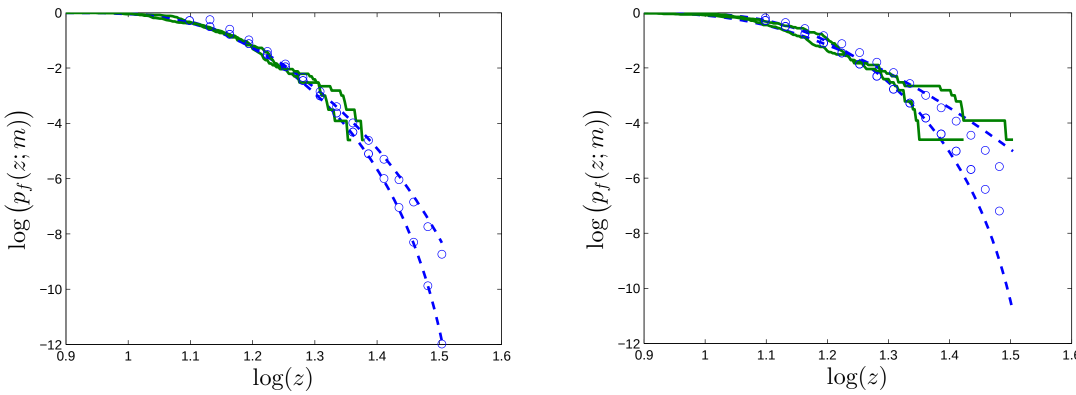

Figure 12: MC (solid lines), GEV (dash lines), and GP (circular markers) estimates of $p_f(z; m)$ for $\{Z_i\}$ defined by Eq. 16 driven by Gaussian white noise for $\rho = 0.0$ (left panel) and $\rho = 0.7$ (right panel)

that are limited to the range of observations, the GEV and GP estimates extend beyond data.

Example 4. Suppose the driving noise $\{W_i\}$ in Eq. 16 follows a shifted marginal exponential with mean 0 and variance 1, so that the time series $\{Z_i\}$ is not Gaussian. The relationships between the skewness and kurtosis coefficients, γ_3 and γ_4, of $\{Z_i\}$ in the stationary regime and the corresponding coefficients, $\gamma_{W,3} = 2$ and $\gamma_{W,4} = 9$, of $\{W_i\}$ are [4] (Example 3.35)

$$\gamma_3 = \frac{(1-\rho^2)^{3/2}}{1-\rho^3}\,\gamma_{W,3} \quad \text{and} \quad \gamma_4 = \frac{6\,\rho^2 + (1-\rho^2)\,\gamma_{W,4}}{1+\rho^2}.$$

For example, the skewness and kurtosis coefficients of $\{Z_i\}$ are $(\gamma_3, \gamma_4) = (1.1087, 5.0537)$ and $(0.6112, 3.6298)$ for $\rho = 0.7$ and $\rho = 0.9$, respectively.

Block maxima model. Samples of block maxima are used, as in the previous case in which the driving noise is Gaussian, to construct GEV approximations for the distribution of M_m. Numerical results are for $m = 1000$. The solid lines in Figs. 13 and 14 are GEV estimates of failure probability $p_f(z; m)$ based on two sets of $n_b = 100$ and $n_b = 1000$ samples of $\{Z_i\}$ with length $m = 1000$ for $\rho = 0.0$ and $\rho = 0.7$. The dash lines are MC estimates obtained from the same observations of $\{Z_i\}$. Previous comments for Gaussian series apply, i.e., the GEV estimates of $p_f(z; m)$ fit data satisfactorily but exhibit notable sample-to-sample variation for relatively small number of blocks. This variation is caused by statistical uncertainty and can be reduced by increasing the number of blocks.

The left and right panels in Fig. 13 show MC and GEV estimates of $p_f(z; m)$ for $\rho = 0.0$ and $\rho = 0.7$, respectively, that are obtained from two sets of $n_b = 100$ blocks of samples of $\{Z_i\}$ with length $m = 1000$. The MLE estimates $(\hat{\mu}_m, \hat{\sigma}_m, \hat{\xi}_m)$ of the GEV distributions for $\rho = 0.0$ and $\rho = 0.7$ are $(5.7436, 0.9070, 0.0627)$ and $(5, 9499, 1.1310, -0.1647)$. The 90% confidence intervals for the estimates $\hat{\mu}_m$, $\hat{\sigma}_m$, and $\hat{\xi}_m$ are $(5.5421, 5.9451)$, $(0.7685, 1.0703)$, and $(-0.0931, 0.2186)$ for one of the data sets and $(5.7023, 6.1974)$, $(0.9681, 1.3213)$, and $(-0.3008, -0.0286)$ for the other. Similar results are for the GEV estimates shown in the

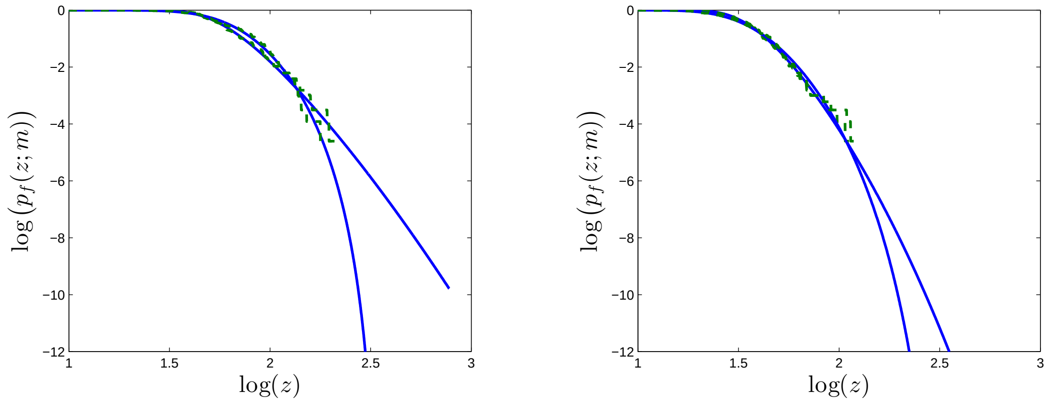

Figure 13: MC (dash lines) and GEV (solid lines) estimates of $p_f(z;m)$ for AR1 state driven by Exponential white noise for $n_b = 100$, $\rho = 0.0$ (left panel) and $\rho = 0.7$ (right panel)

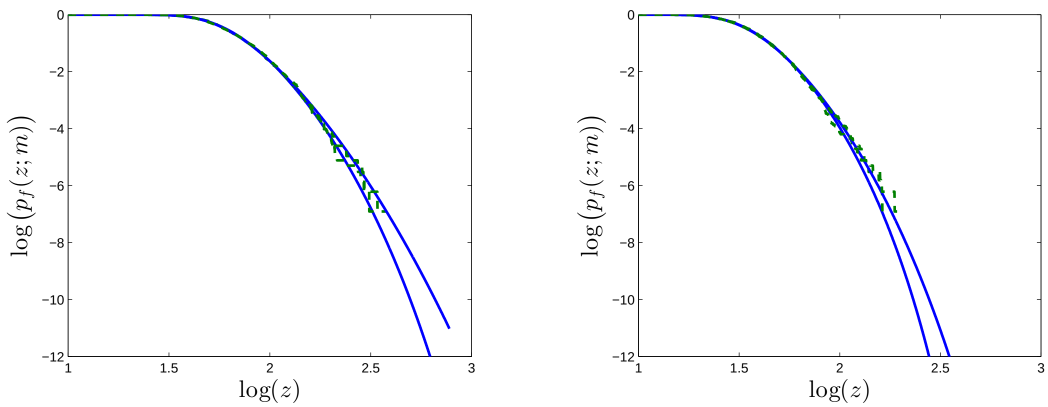

Figure 14: MC (dash lines) and GEV (solid lines) estimates of $p_f(z;m)$ for AR1 state driven by Exponential white noise for $n_b = 1000$, $\rho = 0.0$ (left panel) and $\rho = 0.7$ (right panel)

right panel of the figure. The estimates improve significantly as the sample size is increased from $n_b = 100$ to $n_b = 1000$ blocks, as illustrated in Fig. 14. For example, the MLE estimates of the shape parameter based on two sets of $n_b = 1000$ blocks, $\rho = 0.0$, are $\hat{\xi}_m = -0.0247$ and $\hat{\xi}_m = 0.0187$ with 90% confidence intervals $(-0.0654, 0.0160)$ and $(-0.0281, 0.0655)$. The corresponding estimates for $\rho = 0.7$ are $\hat{\xi}_m = -0.0520$ and $\hat{\xi}_m = -0.0214$ with 90% confidence intervals $(-0.0922, -0.0119)$ and $(-0.0620, 0.0192)$.

Threshold model. Estimates of $p_f(z;m)$ are constructed from single samples of $\{Z_i\}$ with length $n = n_b\, m = 1000000$ corresponding to $n_b = 1000$ sets of samples of $\{Z_i\}$ with size $m = 1000$. MLE estimates $(\hat{\xi}, \hat{\tilde{\sigma}})$ for the parameters $(\xi, \tilde{\sigma})$ of excesses above selected thresholds u_0 assumed to follow GP distributions are constructed as in the previous example. The extremal index is estimated from the observed number $n_{\text{clust}}(z,k)$ of clusters of $\{Z_i\}$ with size $k = 1, 2, \ldots$ above z. A cluster of size k above a level z is defined by k consecutive values of $\{Z_i\}$ above z, e.g., $\{Z_r < z, Z_{r+1} \geq z, \ldots, Z_{r+k} \geq z, Z_{r+k+1} < z\}$ produses such a cluster. Since the estimated average cluster size above z is $\sum_{k\geq 1} k\, n_{\text{clust}}(z,k) / \sum_{k\geq 1} n_{\text{clust}}(z,k)$, we estimate the extremal index by

$$\hat{\eta}(z) = \frac{\sum_{k \geq 1} n_{\mathrm{clust}}(z, k)}{\sum_{k \geq 1} k \, n_{\mathrm{clust}}(z, k)}. \tag{17}$$

The entries in the above definition of $\hat{\eta}(z)$, i.e., the number of clusters $\{n_{\mathrm{clust}}(z, k)\}$ of various sizes k, are obtained by counting from the sample of $\{Z_i\}$. The solid, dash, and dash-dot lines in Fig. 15 are estimates $\hat{\eta}(z)$ for $\rho = 0.0$, 0.7, and 0.9 that are derived from clusters

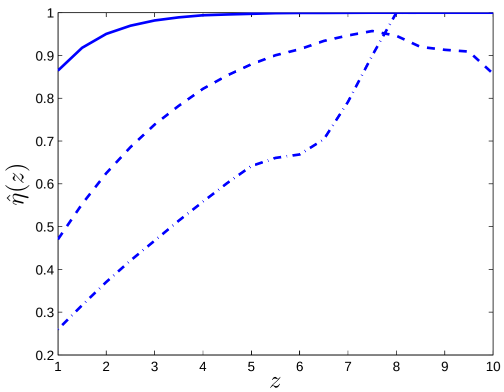

Figure 15: Estimates $\hat{\eta}(z)$ of extremal index for $\rho = 0.0$ (solid line), $\rho = 0.7$ (dash line), and $\rho = 0.9$ (dash-dot line)

of $\{Z_i\}$ above levels z. Since $\hat{\eta}(z)$ increases with z and approaches 1, the extremes of this series do not cluster so that there is no need to correct the estimates of $p_f(z; m)$ constructed under the assumption of independence between extremes of $\{Z_i\}$.

Figure 16 shows MC and GP estimates of $p_f(z; m)$ based on a sample of $\{Z_i\}$ with size

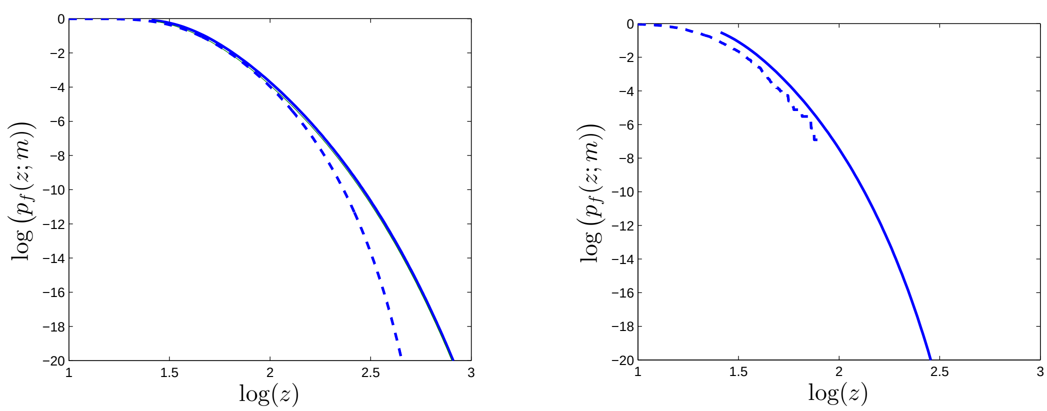

Figure 16: MC (dash lines) and GP (solid lines) estimates of $p_f(z; m)$ based on $n_b = 1000$ blocks with length $m = 1000$ for $\rho = 0.7$ (left panel) and $\rho = 0.9$ (right panel)

$n = n_b \, m = 1000000$ for $\rho = 0.7$ (left panel) and $\rho = 0.9$ (right panel). The dash lines are MC estimates of $p_f(z; m)$. The solid line are GP estimates of $p_f(z; m)$ is obtained under the assumption that extremes of $\{Z_i\}$ do not cluster in agreement with the estimates of extremal indices in Fig. 15. The GP estimates of $p_f(z;m)$ are less satisfactory for $\rho = 0.9$ probably because excesses of $\{Z_i\}$ above the threshold considered in analysis are not independent.

Figure 17 presents results as in Fig. 8 presented at the end of Example 2. It shows,

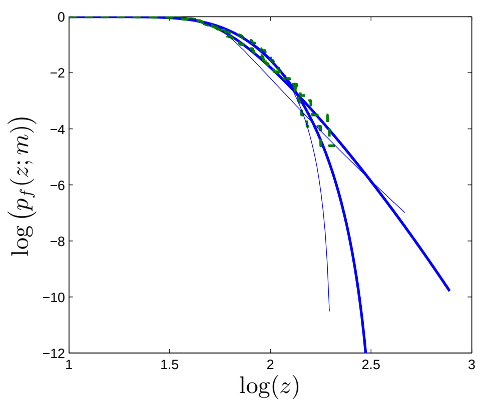

Figure 17: MC (dash lines), GEV (heavy solid lines), and GP (thin solid lines) estimates of $p_f(z;m)$ for AR1 state driven by Exponential white noise for $n_b = 100$, $\rho = 0.0$ (left panel) and $\rho = 0.7$ (right panel)

in addition to the GEV and MC estimates of $p_f(z;m)$ in Fig. 14, GP estimates of this probability in thin solid lines that correspond to $u_0 = 5.9078$. This threshold results from the condition $1 - F(u_0) = n_b/n$, where F is an estimate of the marginal distribution of $\{Z_i\}$, $n_b = 100$, $n = n_b\, m$, and $m = 1000$. For $\rho = 0.0$ the estimates of $(\xi, \tilde{\sigma})$ for the two GP approximation of $p_f(z;m)$ are $(0.1778, 0.6463)$ and $(-0.3228, 1.3360)$ with rather large confidence intervals. As for the estimates by the block model, these estimates stabilize if the sample size is increased from $n = 10^5$ to $n = 10^6$, in which cases they are $(-0.0357, 1.0233)$ and $(-0.0572, 1.0702)$. For $\rho = 0.7$ the estimates of $(\xi, \tilde{\sigma})$ for the two GP approximation of $p_f(z;m)$ are $(0.3536, 0.3637)$ and $(-0.3929, 1.0819)$ with rather large confidence intervals. As for the estimates by the block model, these estimates stabilize if the sample size is increased from $n = 10^5$ to $n = 10^6$, in which cases they are $(0.0485, 0.6705)$ and $(-0.1139, 0.7222)$. The GEV and GP estimates of $p_f(z;m)$ are similar and consistent with MC estimates in the data range but differ for higher thresholds. Results also suggest that the sample size in Fig. 17 needs to be increase to obtain informative estimates of system reliability.

4.3 Displacement of simple oscillators

Suppose $X(t)$ is displacement of single degree of freedom system defined by

$$\ddot{X}(t) + 2\,\zeta_0\,\nu_0\,\dot{X}(t) + \nu_0^2\,X(t) = V(t) \quad t \geq 0, \tag{18}$$

where $\nu_0 > 0$ and $\zeta_0 > 0$ are frequency and damping parameters. The input is $V(t) = Y(t)$ or $V(t) = Y(t)^2$, where $Y(t)$ is an Ornstein-Uhlenbeck process defined by

$$dY(t) = -\lambda\,Y(t)\,dt + \sqrt{2\,\lambda}\,dB(t), \tag{19}$$

and $B(t)$ is a standard Brownian motion.

Our objective is to approximate system reliability $p_s(z;m)$, i.e., the probability that $X(t)$ does not leave a safe set $D_z = (-\infty, z]$, $z > 0$, during a time interval $[0, \tau]$. Since $X(t)$ is recorded at discrete times $\{t_i\}$, this safety condition can only be imposed at a finite number m of times. Accordingly, we calculate $p_s(z;m) = P\big(X(t_i) \in D_z,\ i = 1, \ldots, m\big)$ or, equivalently, $p_s(z;m) = P(M_m \leq z)$, where $M_m = \max(Z_1, \ldots, Z_m)$, $Z_i = X(t_i)$, $t_{i+1} = t_i + \Delta t$, and $\Delta t = 0.1$ denotes the time step.

Example 5. Suppose $X(t)$ denotes the displacement of the linear oscillator in Eq. 18 with $V(t) = Y(t)$. The $\mathbb{R}^3$-valued process $\big(X_1(t) = X(t), X_2(t) = \dot{X}(t), X_3(t) = Y(t)\big)$ becomes stationary as time increases indefinitely. Let $c_{ij}(\tau) = E[X_i(t+\tau)\, X_j(t)]$ and $\gamma_{ij} = c_{ij}(0)$ denote the stationary covariance functions and covariances of this vector process. The stationary covariances are $\gamma_{11} = (\lambda - \beta)\,\delta/(\alpha\,\beta)$, $\gamma_{12} = 0$, $\gamma_{13} = \delta$, $\gamma_{23} = \lambda\,\delta$, $\gamma_{22} = -\lambda\,\delta/\beta$, $\gamma_{33} = 1$, where $\alpha = -\nu_0^2$, $\beta = -2\,\zeta_0\,\nu_0$, and $\delta = 1/(\lambda^2 - \alpha - \beta\,\lambda)$. The covariance function of $X_1(t) = X(t)$ is the solution of $\dot{c}_{11}(\tau) = c_{21}(\tau)$ that depends on $c_{21}(\tau)$ defined $\dot{c}_{21}(\tau) = \alpha\, c_{11}(\tau) + \beta\, c_{21}(\tau) + c_{31}(\tau)$ which involves $c_{31}(\tau)$ defined by $\dot{c}_{31}(\tau) = -\lambda\, c_{31}(\tau)$. The solution of this system of equations with $c_{ij}(0) = \gamma_{ij}$ shows that $c_{11}(\tau) \sim O\big(\exp(-\min(\lambda, \zeta_0\,\nu_0)\,\tau)\big)$ for large $\tau > 0$, so that $c_{11}(\tau)\,\log(\tau) \to 0$ as $\tau \to \infty$. Since $X(t) = X_1(t)$ is a Gaussian process, we conclude that $P\big((M_m - b_m)/a_m \leq z\big) \to \exp\big(-\exp(-z)\big)$, where $\{a_m > 0\}$ and $\{b_m\}$ are the constants for independent Gaussian series given in a previous section [6] (Theorem 4.3.3). In this case, the asymptotic distributions of M_m and M_m^* coincide so that the extremal index is $\eta = 1$. Following are estimates $p_f(z, m)$ obtained by block maxima and threshold models.

Block maxima model. Numerical results in Fig. 18 are for $Z_\tau = \max_{0 \leq t \leq \tau}\{X(t)\}$, $\nu_0 = \pi$, $\zeta_0 = 0.05$, $\lambda = 1$, and $V(t) = Y(t)$. The left and right panels in Fig. 18 show estimates of $p_f(z;\tau)$ based on two sets of $n_b = 100$ independent samples with length $\tau = 10000$,

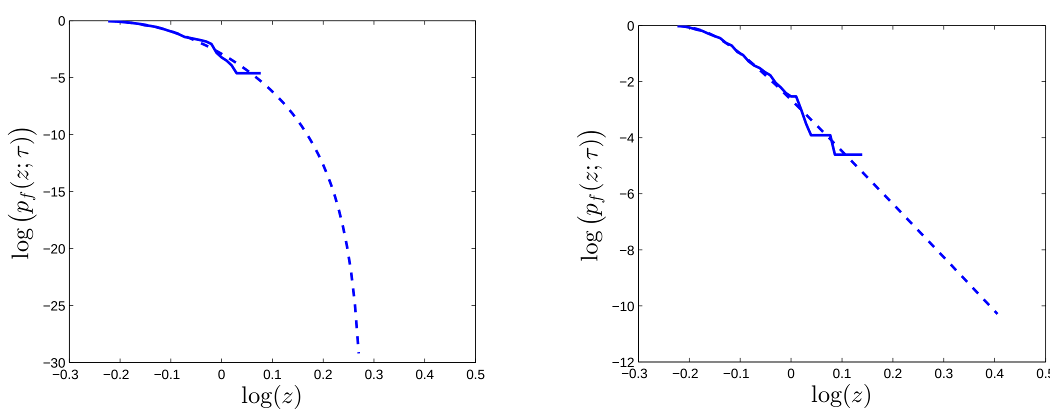

Figure 18: MC (solid lines) and GEV (dash lines) estimates of $p_f(z;\tau)$ for two sets of $n_b = 100$ independent samples of $X(t)$ for $\tau = 10000$ and $D = (-\infty, z]$, $z > 0$

so that the block size coincides with τ. Since $X(t)$ was sampled at every $\Delta t = 0.1$, the length of all time series is $\tau/\Delta t = 100000$. The solid and dash lines are MC and GEV estimates. MC estimates of $p_f(z;\tau)$ extend over the range of data while GEV estimates of this probability can be extended beyond data provided the estimates $(\hat{\mu}, \hat{\sigma}, \hat{\xi})$ of the parameters (μ, σ, ξ) of the asymptotic GEV distributions are accurate. These estimates are $(0.8698, 0.0533, -0.1171)$ and $(0.8677, 0.0476, 0.0476)$ for the plots in the left and right panels. The GEV estimates of $p_f(z; \tau)$ differ significantly because of the large uncertainty in estimates of the shape parameter ξ. The discrepancy between these estimates can be reduced significantly by increasing n_b. Figure 19 shows plots as in Fig. 18 for $n_b = 1000$

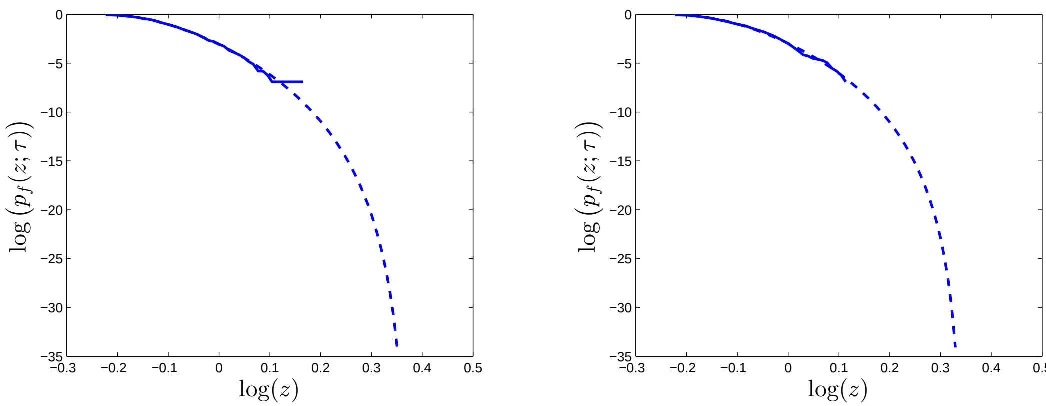

Figure 19: MC (solid lines) and GEV (dash lines) estimates of $p_f(z; \tau)$ for two sets of $n_b = 1000$ independent samples of $X(t)$ for $\tau = 10000$ and $D = (-\infty, z]$, $z > 0$

rather than $n_b = 100$. The corresponding GEV estimates of $p_f(z; m)$ and estimates of the shape parameter ξ, $\hat{\xi} = -0.0853$ and -0.0955, are similar.

Threshold model. Estimates are constructed for $p_f(z; \tau)$ from two samples of $X(t)$ containing the same information as those used to construct the estimates of this probability in Fig. 19. The length of these samples is $\tau\, n_b$ so that there are $\tau\, n_b / \Delta t = 10^8$ observations in each sample since $\tau = 10000$, $n_b = 1000$, and $\Delta t = 0.1$. These samples are used to construct the estimates of $p_f(z; \tau)$ in Fig. 20. Storage of samples of this size demands significant memory particularly when dealing with large dimensional vector state processes.

The solid and dash lines in Fig. 20 are MC and GP estimates of $p_f(z; \tau)$. The GP and MC estimates are consistent and exhibit limited sample-to-sample variation, in agreement with results in Fig. 19. Following considerations in Sect. 3.2.1, a threshold $u_0 = 0.5$ has been used to construct both estimates. The estimates of ξ for the plots in the left and right panels are $\hat{\xi} = -0.0825$ and -0.0874. The corresponding estimates of $\tilde{\sigma}$ are $\hat{\tilde{\sigma}} = 0.0730$ and 0.0731. The 90% confidence intervals on the two estimates of ξ are $(-0.0845, -0.0804)$ and $(-0.0894, -0.0854)$. The 90% confidence intervals on $\hat{\tilde{\sigma}}$ are $(0.0728, 0.0732)$ and $(0.0729, 0.0734)$.

Figure 21 shows, in addition to the estimates of $p_f(z; m)$ in Fig. 20, GP estimates of this probability for $u_0 = 0.87$. This threshold is exceeded by $\{Z_i\}$ approximately $n_b = 1000$ times, so that the excesses of this time series above u_0 matches the number of blocks n_b. The latter estimates, which are plotted in thin solid lines, match MC estimates in the data range but differ from the other GP estimates of $p_f(z; m)$ and the corresponding GEV estimates in Fig. 19.

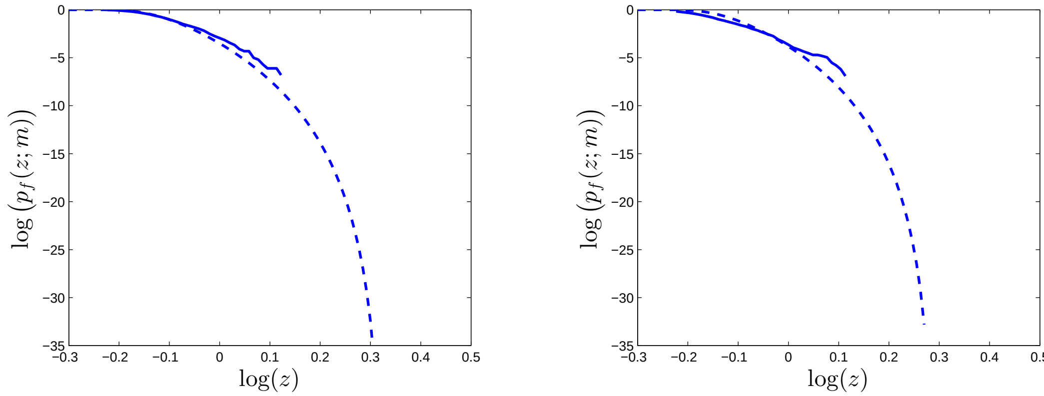

Figure 20: MC (solid lines) and GP (dash lines) estimates of $p_f(z;\tau)$ for two sets of independent samples of $X(t)$ with length $\tau\, n_b$ for $\tau = 10000$ and $n_b = 1000$ and $D = (-\infty, z]$, $z > 0$

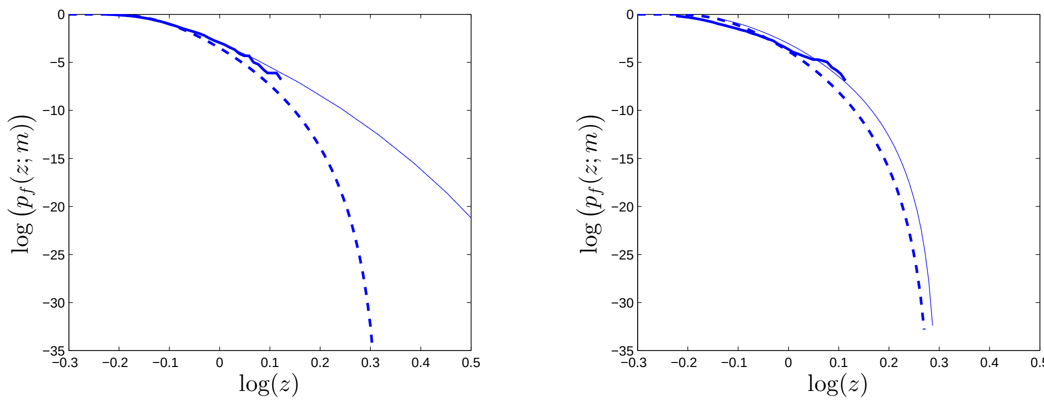

Figure 21: MC (solid lines) and GP (dash lines) estimates of $p_f(z;\tau)$ for two sets of independent samples of $X(t)$ with length $\tau\, n_b$ for $\tau = 10000$ and $n_b = 1000$ and $D = (-\infty, z]$, $z > 0$. This solid lines are GP estimates for $u_0 = 0.87$

Example 6. Suppose the input to the oscillator in Eq. 18 is the square of the Ornstein-Uhlenbeck process in Eq. 19, i.e., $V(t) = Y(t)^2$, so that both $V(t)$ and $X(t)$ are non-Gaussian processes. Our objective is to estimate $p_f(z;\tau) = P\big(Z_\tau > z\big)$ from samples of $X(t)$ similar to those in the previous example by the block maxima and threshold models. Data for these models consists of sets of $n_b = 1000$ samples with length $\tau = 10000$ and single samples with length $\tau\, n_b$ sampled at $\Delta t = 0.1$.

Block maxima model. Figure 22 shows with solid and dash lines MC and GEV estimates of the failure probability $p_f(z;\tau)$ for two sets of $n_b = 1000$ independent samples of $X(t)$ with length $\tau = 10000$. The two panels correspond to two sets of samples. The estimates $(\hat{\mu}, \hat{\sigma}, \hat{\xi})$ of the parameters (μ, σ, ξ) of the asymptotic GEV distributions are $(2.5585, 0.2802, -0.0311)$ and $(2.5489, 0.2752, -0.0170)$ for the plots in the left and right panels. The 90% confidence intervals on the estimates $\hat{\mu}$, $\hat{\sigma}$, and $\hat{\xi}$ of the GEV approximations of $p_f(z;\tau)$ are $(2.5391, 2.5779)$, $(0.2667, 0.2944)$, and $(-0.0740, 0.0118)$ in the left panel and $(2.5298, 2.5680)$, $(0.2618, 0.2892)$,

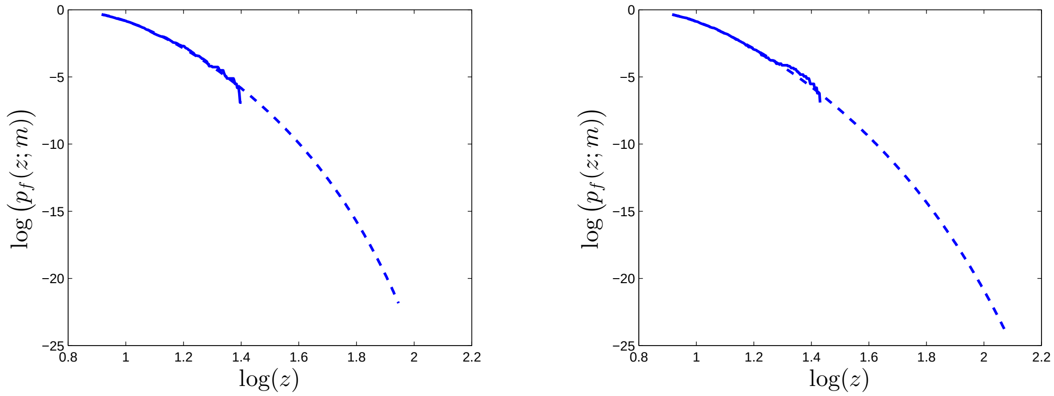

Figure 22: MC (solid lines) and GEV (dash lines) estimates of $p_f(z;\tau)$ for two sets of $n_b = 1000$ independent samples of $X(t)$ with length $\tau = 10000$

and $(-0.0598, 0.0259)$ in the right panel.

As in the previous example, the GEV estimates of $p_f(z;\tau)$ are consistent with MC results within the data range. Also, the GEV estimates of $p_f(z;\tau)$ corresponding to the two data sets are similar for thresholds z much larger than available observations suggesting that they can be used to assess the performance of highly reliable dynamic systems.

Threshold model. The panels in Fig. 23 show estimates of $p_f(z;\tau)$ derived from two samples

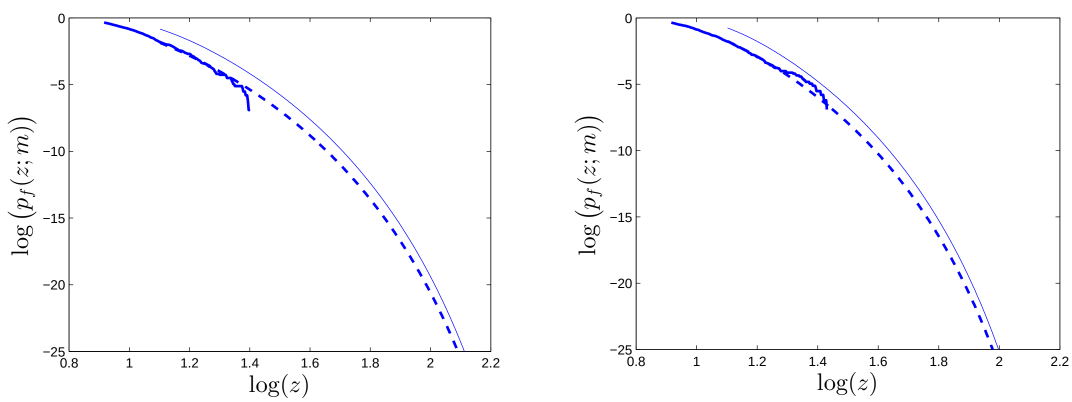

Figure 23: MC (heavy solid lines), GP disregarding clusters (this solid lines), and GP considering clusters (dash lines) estimates of $p_f(z;\tau)$ for two sets of independent samples of $X(t)$ with length $\tau\, n_b$ for $\tau = 10000$ and $n_b = 1000$ and $D = (-\infty, z]$, $z > 0$

of $X(t)$ with length $\tau\, n_b$ for $\tau = 10000$ and $n_b = 1000$, so that they use the same number of observations as the estimates of this probability based on the block maxima model in Fig. 22. As in this figure, the heavy solid lines are MC estimates of $p_f(z;\tau)$. The thin solid and heavy dash lines are GP estimates of $p_f(z;\tau)$ that do not and do account for clustering of extremes via extremal indices. The estimates $(\hat{\xi}, \hat{\tilde{\sigma}})$ of the parameters $(\xi, \tilde{\sigma})$ of the GP distributions in the two panels of Fig. 23 are $(-0.0333, 0.2626)$ and $(-0.0312, 0.3081)$, and have been calculated for $u_0 = 3$. The corresponding 90% confidence intervals are $(-0.1091, 0.0424)$ and

$(-0.1085, 0.0461)$ for $\hat{\xi}$ and $(0.2340, 0.2903)$ and $(0.2754, 0.3447)$ for $\hat{\tilde{\sigma}}$.

Figure 24 shows, in addition to the estimates of $p_f(z;m)$ in Fig. 23, GP estimates of this

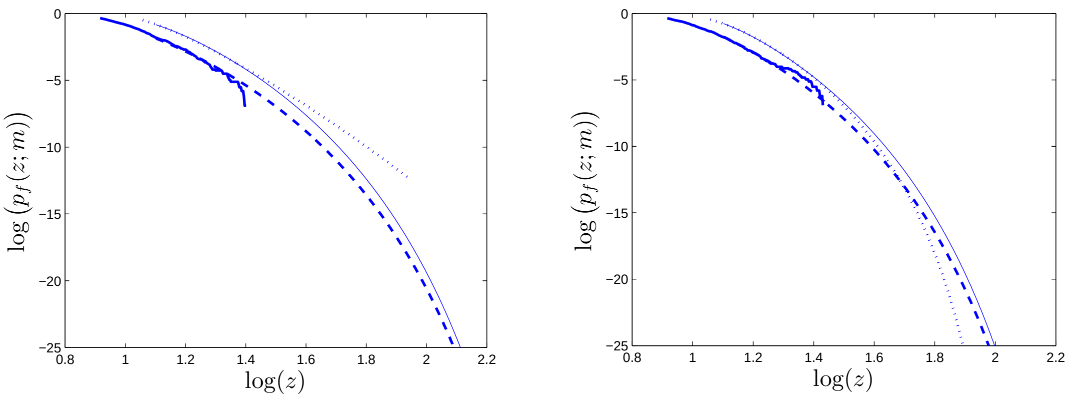

Figure 24: MC (heavy solid lines), GP disregarding clusters (this solid lines), and GP considering extreme clusters (dash lines) estimates of $p_f(z;\tau)$ for two sets of independent samples of $X(t)$ with length $\tau\, n_b$ for $\tau = 10000$ and $n_b = 1000$ and $D = (-\infty, z]$, $z > 0$

probability for a threshold $u_0 = 2.86$ that is exceeded by approximately $n_b = 1000$ observations. The latter estimates of $p_f(z;m)$ are obtained under the assumption that extremes of $\{Z_i\}$ do not cluster and are shown with dot lines. Since these estimates differ from the GP estimates based on thresholds u_0 derived following considerations in Sect. 3.2.1, their versions corrected for clustering are not presented.

The thin solid and heavy dash lines in Figs. 23 and 24 are identical and represent GP estimates of $p_f(z;m)$ that disregard and account for clustering of extremes of $\{Z_i\}$. Since there are no simple criteria for determining whether extremes of non-Gaussian series cluster, we estimated extremal indices from Eq. 17. The left and right panels in Fig. 25 show estimates $\hat{\eta}(z)$ of the extremal index for two independent samples of the Gaussian series in

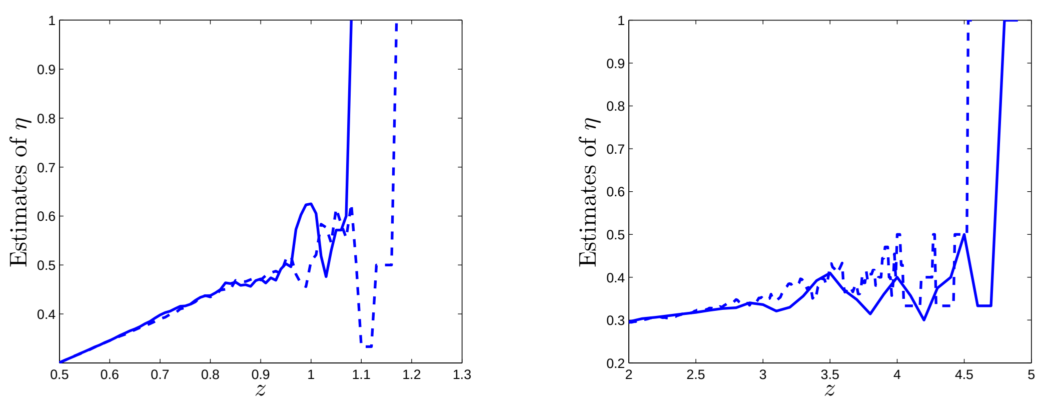

Figure 25: Estimates of extremal indices in Eq. 17 for two samples of $X(t)$ with length $n = 10^8$ under $V(t) = Y(t)$ (left panel) and $V(t) = Y(t)^2$ (right panel)

Example 5 and the non-Gaussian series in this example. The estimates in the left panel increase steadily with z indicating that the extremes of $\{Z_i\}$ in Example 5 do not cluster, in agreement with theoretical arguments. On the other hand, the estimates $\hat{\eta}(z)$ in the right panel seem to reach a plateau, which suggest that the extremes of $\{Z_i\}$ in this example cluster. The corresponding value of the extremal index is equal approximately to $\hat{\eta} = 0.4$. The heavy dash lines in Figs. 23 and 24 are derived from the thin solid lines by the following calculations. Let $p_{f,0}(z;m)$ denote GP estimates of $p_f(z;m)$ obtained under the assumption that the extremes of $\{Z_i\}$ do no cluster. These estimates are shown with solid thin lines. The GP estimates that account for clustering of extremes are given by $1 - \big(1 - p_{f,0}(z;m)\big)^{\hat{\eta}}$. They are shown with heavy dash lines.

We note that the GEV and GP estimates of failure probabilities reported in this study are based on $n_b = 100; 1000$ blocks of length $m = 1000$ for the block model and a single sample of length $n_b\, m = 10^5; 10^6$ for the threshold model. For $n_b = 1000$ and $m = 1000$, these estimates are accurate up failure probabilities of order 10^{-15} to 10^{-20} provided the estimates $\hat{\xi}$ of the shape parameter ξ are not in a small vicinity of zero. In contrast, Monte Carlo estimates of failure probability based on samples of size $n_b\, m = 10^5; 10^6$, i.e., the sample size used to construct GEV and GP estimates, are reliable up to thresholds corresponding to instantaneous failure probabilities of order $10^{-4}; 10^{-5}$. Monte Carlo estimates for failure probabilities of order 10^{-15} would require 10^{16} samples.

5 Conclusions

Generalized extreme value (GEV) and generalized Pareto (GP) distributions fitted to relatively small sets of samples of state processes have been used to estimate the reliability of dynamic systems during a reference time τ. The GEV and GP distributions are fitted to extremes of state processes in τ and excesses of these processes above specified thresholds. Block maxima and threshold models have been used to fit these distributions. The GEV and GP estimates can be used to assess performance of highly-reliable dynamic systems since they extend outside the data range. In contrast, Monte Carlo estimates based on the same observations can only be used to assess the performance of at most moderately-reliable dynamic systems since they are available only within data range.

The computational effort required for implementing the GEV and GP estimates is minimal relative to that for generating state samples for realistic dynamic systems. The GEV estimates have some notable features that made them attractive for system reliability analysis. They are conceptually simple, apply to both stationary and non-stationary states, and require low storage. The GP estimates are conceptually less simple, apply directly to only stationary series, and require relatively high storage. Although both estimates are accurate, the GEV estimates are believe to be preferable for analyzing dynamic systems.

The errors of GEV and GP estimates of system reliability are of two types. The first relates to the assumption that extremes of state processes follow GEV distributions although the reference time is finite. The second type of error relates to the fact that the parameters of the GEV and GP distributions are estimated from finite sets of observations. The first type of error results in biased estimates and cannot be eliminated. The second type of error can be reduced by increasing the sample size. This error can be dominant when the estimates of the shape parameters of the GEV and GP distributions are in a small vicinity of zero.

Numerical examples involving independent/dependent, Gaussian/non-Gaussian time series representing observations of state processes show that the GEV and GP estimates of system reliability are accurate and simple to implement. Confidence intervals and comparisons between reliability estimates based on different sets of observations have been used to quantify the performance of the proposed reliability estimates. Generally, the GEV and GP estimates are accurate and can be used to extend Monte Carlo estimates of failure probabilities several order of magnitude beyond data.

6 Acknowledgements

The work of the first author reported in this paper has been supported by the National Science Foundation under grants CMMI-0969150 and CMMI-1265511. The research of the second authors has been supported by the ARO MURI grant W911NF-12-10385. The support is gratefully acknowledged.

References

[1] S. Asmussen, K. Biswanger, and B. Højgaard. Rare events simulation for heavy-tailed distributions. *Bernoulli*, 6(2):303–322, 2000.

[2] K. W. Breitung. *Asymptotic Approximations for Probability Integrals*. Springer-Verlag, New York, 1994. Lecture Notes in Mathematics, 1592.

[3] S. Coles. *An Introduction to Statistical Modeling of Extreme Values*. Springer, London.

[4] M. Grigoriu. *Applied Non-Gaussian Processes: Examples, Theory, Simulation, Linear Random Vibration, and MATLAB Solutions*. Prentice Hall, Englewoods Cliffs, NJ, 1995.

[5] M. Grigoriu. *Stochastic Calculus. Applications in Science and Engineering*. Birkhäuser, Boston, 2002.

[6] M. R. Leadbetter, G. Lindgren, and H. Rootzén. *Extremes and Related Properties of Random Sequences and Processes*. Springer-Verlag, New York, 1983.

[7] A. Naess and O. Gaidai. Monte Carlo methods for estimating the extreme response of dynamic systems. *Probabilistic Engineering Mechanics*, 2007. submitted.

[8] A. Naess and O. Gaidai. Monte Carlo methods for estimating the extreme response of dynamical systems. *Journal of Engineering Mechanics, ASCE*, 134(8):628–636, 2008.

[9] T. Nguyen and G. Samorodnitsky. Tail inference: where does tail begin? *Extremes*, 15:437–461, 2012.

[10] E. Simiu and N. A. Heckert. Extreme wind distribution tails: A 'peaks over thresold' approach. Technical Report NIST BUILDING SCIENCE SERIES 174, NationalInstituotfeStandardasndTechnolo, GaithersburMgD, 20899-0001, 1995.